Fermi National Accelerator Laboratory

Fermilab–PUB–93/350–T
ETH-TH/93–41

The evolution of parton distributions at small x

R. K. Ellis

Fermi National Accelerator Laboratory,
P. O. Box 500,
Batavia, IL 60510, USA.

Z. Kunszt

Theoretical Physics,
ETH, Hönggerberg,
8093 Zürich, Switzerland.

E. M. Levin [1]

Fermi National Accelerator Laboratory,
P. O. Box 500,
Batavia, IL 60510, USA.

Abstract

We investigate parton distributions at small x using moments of the Gribov-Lipatov-Altarelli-Parisi (GLAP) evolution equation with respect to x. In this representation the kernel of the GLAP equation contains singularities in the moment variable ω at $\omega = 0$. We show that the importance of these singularities at small x depends on the form of the starting distributions. We examine the range of x in which the GLAP equation is valid. The restrictions on the range of x depend on the form of the starting distributions. We investigate whether the GLAP equation can be used to interpolate data in the HERA region. Results are given for the structure function F_2 at small x. A possible method of determining the gluon distribution from F_2 is discussed.

[1] On leave from the Petersburg Nuclear Physics Institute, 188350 Gatchina, Russia

Operated by Universities Research Association Inc. under contract with the United States Department of Energy

1 Introduction

The low x region has received a lot of attention from the theoretical community. In particular, there is an extensive literature[1,2,3] on the prediction of the small x behaviour of structure functions using the Balitskii-Fadin-Kuraev-Lipatov (BFKL) equation[4]. Qualitatively, the BFKL equation predicts a growth of x distributions like

$$xf(x) = x^{-\omega_L} \tag{1}$$

where f is the number density of any species of parton and x is the longitudinal momentum fraction of the parton. In the leading approximation the exponent ω_L is found to be,

$$\omega_L^0 = \frac{4C_A \ln 2}{\pi}\alpha_s(Q_0^2); \quad C_A = 3. \tag{2}$$

However attempts to get quantitative information[5] on low x behaviour at accessible values of Q^2 are thwarted by the sensitivity of the BFKL equation to momentum scales below Q_0. In addition the correct treatment of sub-leading terms in the BFKL equation is unknown. We expect these sub-leading terms to be particularly important[3,6].

The small x region is now of special interest because there are new data[7,8]. The advent of the ep machine HERA has opened a new range in Q^2 and x for the study of deep inelastic scattering (DIS). For the purpose of this paper we shall consider the boundary of the region in which precision measurements of DIS can be performed at HERA to be given by[9,10],

$$\frac{Q^2}{x_B} < 10^5\ \mathrm{GeV}^2,\ Q^2 > 10\ \mathrm{GeV}^2,\ x_B < 0.3 \tag{3}$$

In this equation Q^2 is the four-momentum squared of the virtual photon and x_B is Bjorken's x variable.

The present paper has a modest scope. Because of the difficulties of making quantitative predictions with the BFKL equation, in this paper we shall abandon any attempt to *predict* the behaviour of the structure function at small x. We shall instead try to address a few simple questions about structure functions at small x using the Gribov-Lipatov-Altarelli-Parisi (GLAP) evolution equation[11]. The advantage of the GLAP equation is that the effects of energy-momentum conservation and the running of the coupling constant can be included exactly, at least through two loops. In addition, the theoretical framework for going beyond two loops is completely understood. Small x behaviour using the GLAP equation[2] has previously been investigated in refs. [14,15]. It is appropriate to reconsider these questions because of the new information[16] on anomalous dimensions at small ω. As emphasised in ref. [16], the small ω singularities are especially important for the evolution of the singlet quark distribution, which is the dominant term in F_2 measured at HERA. The questions which we pose are the following:-

1. Is there a range of x in which the evolution of the structure functions is dominated by the small x singularities in the anomalous dimensions? In the language of the Mellin Transform this corresponds to the consideration of only the $\omega = 0$ singularities in the anomalous dimensions.

2. Given the presence of $\omega = 0$ singularities in the anomalous dimension and the present knowledge of them, at what values of x and Q^2 does it make sense to use the GLAP equation implemented with only the low order perturbative terms in the anomalous dimension series?

3. Does it make sense to interpolate the data on DIS throughout the HERA range using only the GLAP evolution equation?

We shall answer these questions using a numerical program to invert the moments of the distribution functions, supplemented by analytic considerations at small ω.

Although we shall abandon the BFKL equation as a source of quantitative information we shall use it extensively as a source of inspiration. We will start with a general form of the initial parton distributions suggested by the BFKL equation.

$$xf(x) = x^{-\omega_0}. \tag{4}$$

In addition we shall borrow the concept of a critical anomalous dimension. We shall assume that the perturbative anomalous dimension (like the Lipatov anomalous dimension) has a critical value, which implicitly defines ω_L at subleading level. For $\omega < \omega_L$ finite order perturbation theory in α_s cannot be used to calculate the anomalous dimension. We shall estimate this ω_L by taking the critical anomalous dimension to be one half

$$p^{GG}(\omega_L) = \frac{1}{2}. \tag{5}$$

[2]Following standard practice we shall refer to this equation as the GLAP equation, although in moment space (which we use in this paper) it was also written down by Georgi and Politzer[12] and Gross and Wilczek[13].

We shall find that if $\omega_0 > \omega_L$ with ω_L defined as in Eq. (5), the use of the GLAP equation is justified. In this region we can use the perturbative expansion of the anomalous dimension. On the other hand if the dominant value of ω is less than ω_L, the perturbative anomalous dimension with a finite number of terms will be inadequate.

The plan of the paper is as follows. The solution of the GLAP equation in moment space is presented in section 2. In addition in section 2 we discuss the form of the GLAP kernels at small ω. The results of our full numerical solution of the GLAP equation in various approximations are presented in section 3. The method relies on the numerical evaluation of the inverse Mellin transform in the complex ω plane. This method was pioneered in ref. [17]. Our numerical program is a descendant of the DFLM[18] program to invert the structure functions. The calculation of the evolution using moments of the parton distributions followed by numerical inversion is an efficient and accurate method of solving the GLAP equation. Section 4 investigates the features of the solution at small x using analytic methods. Section 5 presents results on the structure function F_2 in the HERA region. A possible method to extract the gluon distribution function from data on F_2 is discussed in Section 6. Conclusions are presented in Section 7.

2 The GLAP equation and its solution

In this section we describe the evolution of the non-singlet and singlet distributions predicted by the GLAP equation. In the latter case the formalism will be general enough to include three and four loop anomalous dimensions. This is necessary because we want to include information on the small ω behaviour of the anomalous dimensions in three and four loops. It will also be useful if and when the complete three and four loop anomalous dimensions are calculated. The solution is derived as a perturbation about the lowest order result. To make the notation more compact we introduce the following notation for the running coupling,

$$a = \frac{\alpha_s}{2\pi}. \tag{6}$$

This coupling obeys the renormalization group equation,

$$\frac{da}{d\ln Q^2} = -b_0 a^2 - b_1 a^3 - b_2 a^4 - b_3 a^5 + O(a^6) \tag{7}$$

where in the $\overline{MS}$ scheme we have[19],

$$
\begin{aligned}
b_0 &= (11 - \frac{2}{3}f)/2 \\
b_1 &= (102 - \frac{38}{3}f)/4 \\
b_2 &= (\frac{2857}{2} - \frac{5033}{18}f + \frac{325}{54}f^2)/8
\end{aligned} \tag{8}
$$

and f is the number of active flavours. Since b_3 is unknown we will set it equal to zero in our numerical work.

We will formulate the GLAP equation in the space of moments defined as follows. For any function $f(x)$, define the moments $f(\omega)$ as

$$
f(\omega) = \int_0^1 dx\, x^\omega f(x). \tag{9}
$$

In the following we will use f as a generic notation for any parton distribution, *e.g.* u, d, s, c, b, t, G. Note that the moment variable ω is chosen so that the $\omega = 0$ moment measures the number of partons, and the $\omega = 1$ moment measures their momentum. An alternative moment variable N defined such that $N = \omega + 1$ is often found in the literature. In moment space convolutions become products. The GLAP evolution equations for the quark, antiquark and gluon densities are,

$$
\begin{aligned}
\frac{dq_i(\omega)}{d\ln Q^2} &= \left[\sum_k \left\{P_{q_iq_k}(\omega)q_k(\omega) + P_{q_i\bar{q}_k}(\omega)\bar{q}_k(\omega)\right\} + P_{q_iG}(\omega)G(\omega)\right] \\
\frac{d\bar{q}_i(\omega)}{d\ln Q^2} &= \left[\sum_k \left\{P_{\bar{q}_iq_k}(\omega)q_k(\omega) + P_{\bar{q}_i\bar{q}_k}(\omega)\bar{q}_k(\omega)\right\} + P_{\bar{q}_iG}(\omega)G(\omega)\right] \\
\frac{dG(\omega)}{d\ln Q^2} &= \left[\sum_k \left\{P_{Gq_k}(\omega)q_k(\omega) + P_{G\bar{q}_k}(\omega)\bar{q}_k(\omega)\right\} + P_{GG}(\omega)G(\omega)\right]
\end{aligned} \tag{10}
$$

The GLAP kernels P are calculable as a perturbation series in α_s. The solution of these equations is given in the following subsections.

2.1 Non-singlet equation

In this subsection we present the solution of the non-singlet equation in two loops[18]. The solution in this form is used in our numerical evolution program.

The separation of Eq. (10) into singlet and non-singlet parts depends on the properties of the kernel. Using $SU(f)$ flavour symmetry we may define the following combinations of qq and $q\bar{q}$ matrix elements.

$$\begin{aligned}
P_{q_i q_k} &= \delta_{ik} P^V_{qq} + P^S_{qq} \\
P_{q_i \bar{q}_k} &= \delta_{ik} P^V_{q\bar{q}} + P^S_{q\bar{q}} \\
P^{\pm} &= P^V_{qq} \pm P^V_{q\bar{q}}
\end{aligned} \tag{11}$$

In addition, because of charge conjugation invariance and $SU(f)$ flavour symmetry we have that,

$$\begin{aligned}
P_{q_i q_j} &= P_{\bar{q}_i \bar{q}_j} \\
P_{q_i \bar{q}_j} &= P_{\bar{q}_i q_j} \\
P_{q_i G} &= P_{\bar{q}_i G} \equiv P_{qG} \\
P_{G q_i} &= P_{G \bar{q}_i} \equiv P_{Gq}.
\end{aligned} \tag{12}$$

The non-singlet combinations are found to have no $\omega = 0$ singularities[16]. This is easy to understand since the $\omega = 0$ singularities come from the exchange of two gluons in the crossed channel, which cannot occur in non-singlet combinations. In the absence of any special enhancement in three or four loops, we shall perform the evolution of the non-singlet combinations in two loops only. At two loop order, there is a non-zero contribution from P^S_{qq} and $P^S_{q\bar{q}}$, but we have the additional relation

$$P^S_{qq} = P^S_{q\bar{q}}. \tag{13}$$

which simplifies the treatment of the non-singlet pieces.

We now define the sums and differences of the quark and anti-quark distributions as follows,

$$q_i^{\pm} = q_i \pm \bar{q}_i \tag{14}$$

In terms of $q^{\pm}$ we can define the following non-singlet combinations

$$\begin{aligned}
V_i &= q_i^- \\
T_3 &= u^+ - d^+ \\
T_8 &= u^+ + d^+ - 2s^+ \\
T_{15} &= u^+ + d^+ + s^+ - 3c^+ \\
T_{24} &= u^+ + d^+ + s^+ + c^+ - 4b^+ \\
T_{35} &= u^+ + d^+ + s^+ + c^+ + b^+ - 5t^+
\end{aligned} \tag{15}$$

where u, d, s, c, b, t are the distributions of the various species of quarks. To simplify the solution of the equation we introduce the variable t,

$$t = \frac{1}{b_0} \ln \left(\frac{a(Q_0^2)}{a(Q^2)} \right) \tag{16}$$

Q_0 is the starting point of the evolution at which we specify the initial parton distributions. We may expand the kernel of Eq. (10) in a series expansion in powers of a,

$$P^{\pm} = aP_0 + a^2 P_1^{\pm} + O(a^3). \tag{17}$$

Using Eqs. (11,12,13) we find in two loop order,

$$\begin{aligned} \frac{dV_i(\omega,t)}{dt} &= \left[P_0(\omega) + a\left[P_1^-(\omega) - \frac{b_1}{b_0}P_0(\omega)\right]\right]V_i(\omega,t) \\ &\equiv \left[P_0(\omega) + aR^-(\omega)\right]V_i(\omega,t) \end{aligned} \tag{18}$$

$$\begin{aligned} \frac{dT_i(\omega,t)}{dt} &= \left[P_0(\omega) + a\left[P_1^+(\omega) - \frac{b_1}{b_0}P_0(\omega)\right]\right]T_i(\omega,t) \\ &\equiv \left[P_0(\omega) + aR^+(\omega)\right]T_i(\omega,t) \end{aligned} \tag{19}$$

The solution to the non-singlet equations in two loops is[3],

$$V(\omega,t) = \left[1 - (a - a_0)\frac{R^-(\omega)}{b_0}\right] \exp\left(P_0(\omega)t\right)V_i(\omega,0) \tag{20}$$

$$T_i(\omega,t) = \left[1 - (a - a_0)\frac{R^+(\omega)}{b_0}\right] \exp\left(P_0(\omega)t\right)T_i(\omega,0) \tag{21}$$

Our treatment of flavour thresholds follows ref. [18]. For example, below the threshold for bottom quark production, $Q^2 = m_b^2$, the distribution T_{24} evolves as a singlet distribution. Above the bottom threshold it evolves according to Eq. (21). The treatment of singlet evolution is described in the next section.

[3] Eqs. (20,21) correct Eqs. (3.12) and (3.13) of ref.[18].

2.2 The singlet equation

The singlet Altarelli-Parisi equation is

$$\frac{d}{d\ln Q^2}\begin{pmatrix}\Sigma(\omega,Q^2)\\ G(\omega,Q^2)\end{pmatrix}=\begin{pmatrix}P^{FF} & P^{FG}\\ P^{GF} & P^{GG}\end{pmatrix}\begin{pmatrix}\Sigma(\omega,Q^2)\\ G(\omega,Q^2)\end{pmatrix} \tag{22}$$

where $G(\omega)$ is the moment of the gluon distribution and $\Sigma(\omega)$ is the singlet quark combination,

$$\Sigma(\omega,Q^2)=\sum_f q_i^+(\omega,Q^2)\equiv\sum_f\left[q_i(\omega,Q^2)+\bar{q}_i(\omega,Q^2)\right] \tag{23}$$

The elements of the anomalous dimension matrix are given in terms of the kernels defined in Eqs. (11,12) as,

$$\begin{aligned}P^{FF} &= P^+ + f(P^S_{qq}+P^S_{q\bar{q}})\\ P^{FG} &= 2fP_{qG}\\ P^{GF} &= P_{Gq}.\end{aligned} \tag{24}$$

To deal with the singlet equation it is convenient to introduce a matrix notation. We denote matrices by symbols in boldface. Thus the singlet parton distributions may be written as a vector $\mathbf{F}$,

$$\mathbf{F}=\begin{pmatrix}\Sigma\\ G\end{pmatrix} \tag{25}$$

We may expand the matrix kernel in Eq. (22) in powers of a

$$\mathbf{P}=a\mathbf{P_0}+a^2\mathbf{P_1}+a^3\mathbf{P_2}+a^4\mathbf{P_3} \tag{26}$$

where $\mathbf{P_0}$ and $\mathbf{P_1}$ are known completely[22,23]. A partial result on $\mathbf{P_2}$ in the small ω limit has recently been presented[16]. Information on $\mathbf{P_3}$ near $\omega=0$ can be obtained from the kernel of the BFKL equation[24].

Using Eq. (16) we substitute the variable t into the Eq. (22). In matrix notation the singlet equation including terms up to four loop order becomes

$$\frac{d\mathbf{F}(\omega,t)}{dt}=\Big[\mathbf{R_0}(\omega)+a\mathbf{R_1}(\omega)+a^2\mathbf{R_2}(\omega)+a^3\mathbf{R_3}(\omega)\Big]\mathbf{F}(\omega,t) \tag{27}$$

where

$$
\begin{aligned}
\mathbf{R}_0 &= \mathbf{P}_0 \\
\mathbf{R}_1 &= \mathbf{P}_1 - \frac{b_1}{b_0}\mathbf{R}_0 \\
\mathbf{R}_2 &= \mathbf{P}_2 - \frac{b_1}{b_0}\mathbf{R}_1 - \frac{b_2}{b_0}\mathbf{R}_0 \\
\mathbf{R}_3 &= \mathbf{P}_3 - \frac{b_1}{b_0}\mathbf{R}_2 - \frac{b_2}{b_0}\mathbf{R}_1 - \frac{b_3}{b_0}\mathbf{R}_0.
\end{aligned}
\tag{28}
$$

We now present the solution to the singlet equation, which is a generalization of the solutions given in refs.[21,18]. The eigenvalues of the lowest order anomalous dimension, $\mathbf{P}_0$, are

$$
\lambda_\pm = \frac{1}{2}\Big[P_0^{FF} + P_0^{GG} \pm \sqrt{(P_0^{FF} - P_0^{GG})^2 + 4P_0^{FG}P_0^{GF}}\Big] \tag{29}
$$

To obtain a compact matrix solution of the singlet equation we define projection operators in terms of $\lambda_\pm$,

$$
\begin{aligned}
\mathbf{P}_0 &= \lambda_+\mathbf{M}_+ + \lambda_-\mathbf{M}_- \\
\mathbf{M}_+ &= \frac{1}{\lambda_+ - \lambda_-}(\mathbf{P}_0 - \lambda_-\mathbf{1}) \\
\mathbf{M}_- &= \frac{1}{\lambda_+ - \lambda_-}(\lambda_+\mathbf{1} - \mathbf{P}_0)
\end{aligned}
\tag{30}
$$

where $\mathbf{1}$ is the unit matrix. The projection operators $\mathbf{M}_+$ and $\mathbf{M}_-$ satisfy the relations,

$$
\begin{aligned}
\mathbf{M}_+\mathbf{M}_+ = \mathbf{M}_+, &\qquad \mathbf{M}_-\mathbf{M}_- = \mathbf{M}_- \\
\mathbf{M}_+\mathbf{M}_- = \mathbf{M}_-\mathbf{M}_+ = 0, &\quad \mathbf{M}_+ + \mathbf{M}_- = \mathbf{1}.
\end{aligned}
\tag{31}
$$

We shall find a solution of the full singlet equation as a perturbation about the lowest order solution,

$$
\mathbf{F}(\omega,t) = \mathbf{U}(a)\Big(\mathbf{M}_+\exp(\lambda_+ t) + \mathbf{M}_-\exp(\lambda_- t)\Big)\mathbf{U}^{-1}(a_0)\mathbf{F}(\omega,0) \tag{32}
$$

where a_0 is the value of the coupling constant at the starting value $t = 0$. The matrix $\mathbf{U}$ has the expansion

$$
\mathbf{U}(a) = \mathbf{1} + a\mathbf{U}_1 + a^2\mathbf{U}_2 + a^3\mathbf{U}_3 \tag{33}
$$

Substituting $\mathbf{U} = \mathbf{1}$ in Eq. (32) we obtain the lowest order solution. Since by assumption perturbation theory is valid at the starting point, Q_0, the inversion of the matrix $\mathbf{U}$ may also be performed perturbatively,

$$\mathbf{U}^{-1}(a_0) = \mathbf{1} - a_0\mathbf{U_1} - a_0^2(\mathbf{U_2} - \mathbf{U_1}^2) - a_0^3(\mathbf{U_3} - \mathbf{U_1}\mathbf{U_2} - \mathbf{U_2}\mathbf{U_1} + \mathbf{U_1}^3) \quad (34)$$

The explicit forms for the matrices $\mathbf{U_1}, \mathbf{U_2}$ and $\mathbf{U_3}$ which satisfy Eq. (27) are $(\mathrm{j} = 1, 2, 3)$

$$\begin{aligned} \mathbf{U_j} = & -\tfrac{1}{\mathrm{j}b_0}\mathbf{M_+}\mathbf{R'_j}\mathbf{M_+} + \tfrac{1}{\lambda_+ - \lambda_- - \mathrm{j}b_0}\mathbf{M_-}\mathbf{R'_j}\mathbf{M_+} \\ & -\tfrac{1}{\mathrm{j}b_0}\mathbf{M_-}\mathbf{R'_j}\mathbf{M_-} - \tfrac{1}{\lambda_+ - \lambda_- + \mathrm{j}b_0}\mathbf{M_+}\mathbf{R'_j}\mathbf{M_-} \end{aligned} \quad (35)$$

with $\mathbf{R'_1} = \mathbf{R_1}, \mathbf{R'_2} = \mathbf{R_2} + \mathbf{R_1}\mathbf{U_1}$ and $\mathbf{R'_3} = \mathbf{R_3} + \mathbf{R_2}\mathbf{U_1} + \mathbf{R_1}\mathbf{U_2}$.

Dropping terms of higher order in perturbation theory, Eq. (32) may be expanded to give,

$$\begin{aligned} \mathbf{F}(\omega, t) = \Bigg\{ \sum_{\mathrm{k}=\pm} \Big(& \mathbf{M_k} + a\mathbf{U_1}\mathbf{M_k} - a_0\mathbf{M_k}\mathbf{U_1} \\ & + a^2\mathbf{U_2}\mathbf{M_k} - aa_0\mathbf{U_1}\mathbf{M_k}\mathbf{U_1} + a_0^2(\mathbf{M_k}\mathbf{U_1}^2 - \mathbf{M_k}\mathbf{U_2}) \\ & + a^3\mathbf{U_3}\mathbf{M_k} - a^2a_0\mathbf{U_2}\mathbf{M_k}\mathbf{U_1} + aa_0^2(\mathbf{U_1}\mathbf{M_k}\mathbf{U_1}^2 - \mathbf{U_1}\mathbf{M_k}\mathbf{U_2}) \\ & + a_0^3(\mathbf{M_k}\mathbf{U_1}\mathbf{U_2} + \mathbf{M_k}\mathbf{U_2}\mathbf{U_1} - \mathbf{M_k}\mathbf{U_3} - \mathbf{M_k}\mathbf{U_1}^3)\Big) \exp(\lambda_\mathrm{k} t) \Bigg\} \mathbf{F}(\omega, 0). \end{aligned} \quad (36)$$

This equation will be the basis of our numerical solution of the singlet evolution equation.

2.3 Singlet anomalous dimensions at small ω.

Let us consider the defining equation for moments

$$f(\omega) = \int_0^1 dx x^\omega f(x) \equiv \int_0^\infty dy \exp(-\omega y)[x f(x)]; \quad y = \ln(1/x). \quad (37)$$

From Eq. (37) one can see that the variable ω is conjugate to $\ln(1/x)$ so that the behaviour at low x is determined by small ω. We are therefore led to consider the behaviour of the anomalous dimensions at small ω. In this limit we need only consider the singlet distribution.

It is important to establish at the outset the size of ω relative to the other small parameter of the problem, α_s. We shall consider the limit

$$\alpha_s(Q_0^2) \ll \sqrt{\alpha_s(Q_0^2)} \leq \omega \ll 1. \tag{38}$$

Eq. (38) defines a regime in which we can expand perturbatively in both ω and α_s. In this limit we may consistently include higher order terms. Thus if we consider $\omega \sim \epsilon$ and $\alpha_s \sim \epsilon^2$ we shall retain all terms of order ϵ^4 and less. With this value of ω, we shall take into account the following terms in the anomalous dimension series,

$$\begin{array}{ccccl} \epsilon & \epsilon^2 & \epsilon^3 & \epsilon^4 & \\ \alpha_s/\omega, & \alpha_s, & \alpha_s\omega, & \alpha_s\omega^2 & : \mathbf{P_0} \\ & & \alpha_s^2/\omega, & \alpha_s^2 & : \mathbf{P_1} \\ & & & \alpha_s^3/\omega^2 & : \mathbf{P_2} \\ & & & \alpha_s^4/\omega^4 & : \mathbf{P_3} \end{array} \tag{39}$$

In setting up the limit in Eq. (38) we are thinking of a regime where $\alpha_s \approx \frac{1}{4}$ and $\omega \approx \frac{1}{2}$. The choice of α_s as the important parameter rather than the coupling a, (*cf.* Eq. (6)) is a statement about the size of the numerical coefficients which will be justified by the detailed numerical work which follows. Since in this case $\epsilon \sim \frac{1}{2}$ it is clear that the limit in Eq. (38) can only be of marginal validity.

We shall now discuss the value of $\mathbf{P}$ in the small ω limit. The matrix elements of the complete $\mathbf{P_0}$ are well known[20]. In our notation they can be written as,

$$\begin{aligned} P_0^{FF} &= C_F\Big(\frac{3}{2} - \frac{1}{\omega+1} - \frac{1}{\omega+2} - 2S_1(\omega)\Big) \\ P_0^{GF} &= C_F\Big(\frac{2}{\omega} - \frac{2}{\omega+1} + \frac{1}{\omega+2}\Big) \\ P_0^{FG} &= 2T_Rf\Big(\frac{2}{\omega+3} - \frac{2}{\omega+2} + \frac{1}{\omega+1}\Big) \\ P_0^{GG} &= 2C_A\Big(\frac{11}{12} + \frac{1}{\omega} - \frac{2}{\omega+1} + \frac{1}{\omega+2} - \frac{1}{\omega+3} - S_1(\omega)\Big) - \frac{2T_Rf}{3} \end{aligned} \tag{40}$$

where

$$S_1(\omega) = \sum_{j=1}^{\omega} \frac{1}{j} \equiv \psi(\omega+1) - \psi(1). \tag{41}$$

The Casimir operators of colour $SU(3)$ are defined by,

$$C_A = 3, \ \ C_F = \frac{4}{3}, \ \ T_R = \frac{1}{2}. \tag{42}$$

The expansion of Eq. (40) through to order ω^2 as required by Eq.(39) is easily derived. Here we only give the first two terms to show the structure of the matrix in the small ω limit.

$$\mathbf{P_0}(\omega) \to \frac{2}{\omega}\begin{pmatrix} 0 & 0 \\ C_F & C_A \end{pmatrix} + \frac{1}{6}\begin{pmatrix} 0 & 8T_R f \\ -9C_F & -11C_A - 4T_R f \end{pmatrix} + O(\omega) \qquad (43)$$

Note that the quark distribution is fed only by the upper two elements which occur at order ω^0 and higher.

In the next order (in the $\overline{MS}$ scheme), the full result for $\mathbf{P_1}$, defined in Eq. (26) is known[22,23].

$$\mathbf{P_1}(\omega) = \begin{pmatrix} P_1^{FF} & P_1^{FG} \\ P_1^{GF} & P_1^{GG} \end{pmatrix} \qquad (44)$$

In the limit $\omega \to 0$ we have

$$\begin{aligned}
P_1^{FF} &\to \frac{40C_F f T_R}{9\omega} + C_F(C_F - \frac{C_A}{2})(\frac{13}{2} - 6\zeta(2) + 4\zeta(3)) - \frac{317}{27}C_F f T_R \\
P_1^{FG} &\to \frac{40C_A f T_R}{9\omega} + f T_R(2C_F - \frac{134}{9}C_A + \frac{8}{3}\zeta(2)C_A) \\
P_1^{GF} &\to \frac{9C_F C_A - 40C_F f T_R}{9\omega} + C_F^2(6\zeta(2) - 4\zeta(3) - 9) \\
&\quad + C_F C_A(\frac{3637}{108} - \frac{31}{3}\zeta(2) - 6\zeta(3)) + C_F f T_R(1 + \frac{8}{3}\zeta(2)) \\
P_1^{GG} &\to \frac{12C_F f T_R - 46C_A f T_R}{9\omega} \\
&\quad + f T_R(-\frac{61}{9}C_F + \frac{172}{27}C_A) + C_A^2(\frac{1643}{54} - \frac{22}{3}\zeta(2) - 8\zeta(3)). \qquad (45)
\end{aligned}$$

Note that all four entries contain a term of order $1/\omega$ and that the lower components are negative in the small ω limit. For four flavours the matrix becomes,

$$\mathbf{P_1}(\omega) \to \frac{1}{\omega}\begin{pmatrix} 11.8 & 26.7 \\ -7.85 & -27.1 \end{pmatrix} + \begin{pmatrix} -31.6 & -57.7 \\ 45.2 & 98.9 \end{pmatrix} + O(\omega). \qquad (46)$$

The full expression in moment space which we use in our numerical program can be found in ref. [22]. Note the alternating sign in Eq. (46). Comparison of the small ω expansion with the full expression shows that the former is only trustworthy for $\omega \leq 0.3$.

In the next order (in the $\overline{MS}$ scheme) and in the limit $\omega \to 0$ we have[16]

$$\mathbf{P_2}(\omega) \to \frac{224 C_A T_R f}{27\omega^2} \begin{pmatrix} C_F & C_A \\ -C_F\delta & -C_A\eta \end{pmatrix} \tag{47}$$

where δ and η are as yet uncalculated constants. We stress that the magnitude of the constants δ and η is completely unknown. However for $\delta = 1, \eta = 1$ the momentum sum rule is satisfied by the $1/\omega^2$ term alone. The choice of the coefficients of δ and η in Eq. (47) represents a first guess about their size. Lastly we have[24]

$$\mathbf{P_3}(\omega) \to \frac{32 C_A^3 \zeta(3)}{\omega^4} \begin{pmatrix} 0 & 0 \\ C_F & C_A \end{pmatrix} \tag{48}$$

This completes the information we need to perform our numerical analysis consistently in the limit Eq. (38) retaining terms of order ϵ^4.

Since in practice we will be interested in ω not too close to zero the behaviour of the anomalous dimensions at the point $\omega = 1$ is also interesting. For the first two orders, for which we have complete information, the results are,

$$\mathbf{P_0}(\omega) \to \frac{2}{3} \begin{pmatrix} -2C_F & fT_R \\ 2C_F & -fT_R \end{pmatrix} \tag{49}$$

$$\mathbf{P_1}(\omega) \to \frac{1}{54} \begin{pmatrix} 4C_F(14C_F - 47C_A + 26 fT_R) & fT_R(74C_F + 35C_A) \\ -4C_F(14C_F - 47C_A + 26fT_R) & -fT_R(74C_F + 35C_A) \end{pmatrix} \tag{50}$$

Both matrices have the structure required by momentum conservation. Comparison of Eq. (49) and Eq. (43) shows that the anomalous dimensions vary rapidly between $\omega = 0$ and $\omega = 1$.

In practice since $\mathbf{P_0}$ and $\mathbf{P_1}$ are known completely the full expressions will be used in place of their expansions in ω. Note that the full inclusion of $\mathbf{P_0}$ and $\mathbf{P_1}$ without $\mathbf{P_2}$ and $\mathbf{P_3}$ is the standard two loop expression as used in most next-to-leading programs. This is correct to order ϵ^3. Thus one of the new features of this paper is the inclusion of $\mathbf{P_2}$ and $\mathbf{P_3}$.

3 Numerical program

The x space distributions can be reconstructed by considering the inverse Mellin transform.

$$x f(x,t) = \frac{1}{2\pi i} \int_C d\omega \; x^{-\omega} f(\omega, t) \tag{51}$$

The contour of integration C is taken to the right of all singularities. The functions $f(\omega,t)$ are taken to be the solutions to the GLAP equation given in Eqs. (20,21,36).

Our program is available on request[4]. It is a generalization of the DFLM program[18]. In addition to the inclusion of three and four loop effects, we have corrected minor errors in the numerical evaluation of the two loop anomalous dimension matrix and implemented a numerical procedure to choose the contour of integration.

We now report on the results for the evolution of the singlet and gluon distribution functions in the proton. We first define the starting distributions from which we evolve. The valence and sea quark distributions are,

$$\begin{aligned} V_{ud}(x) &= u(x)-\bar{u}(x)+d(x)-\bar{d}(x) && (52)\\ S(x) &= 2(\bar{u}(x)+\bar{d}(x)+\bar{s}(x)+\bar{c}(x)+\ldots). && (53)\end{aligned}$$

The singlet quark distribution is thus given by,

$$\Sigma(x)=V_{ud}(x)+S(x)=\sum_f\left[q_i(x)+\bar{q}_i(x)\right] \tag{54}$$

The initial parton densities are the MRS distributions taken from Martin, Roberts and Stirling[28]. We have considered the two distributions D_0' and D_-' which have differing behaviour at small x. In their notation the two distribution functions have the following forms at the starting value Q_0^2,

$$\begin{aligned} xg(x,Q_0^2) &= A_g x^{\lambda_g}(1-x)^{\eta_g}(1+\gamma_g x) && (55)\\ xV_{ud}(x,Q_0^2) &= A_{ud}x^{\eta_1}(1-x)^{\eta_2}(1+\epsilon_{ud}\sqrt{x}+\gamma_{ud}x) && (56)\\ xS(x,Q_0^2) &= A_s x^{\lambda_S}(1-x)^{\eta_S}(1+\epsilon_S\sqrt{x}+\gamma_S x). && (57)\end{aligned}$$

The coefficients at $Q_0^2=4\ \mathrm{GeV}^2$ taken from ref. [28] are given in Table 1.

The results of the evolution are presented in four approximations. The first is the leading order evolution(L), the second is the complete next to leading order evolution (NL), the third contains the partial results on the next-to-next-to leading evolution (NNL) and the last contains the partial results on four loop anomalous dimension (NNNL) derived from the BFKL equation. In the NNL approximation we have taken $\eta=1$ and $\delta=1$ in the three loop anomalous

[4]From ellis@fnalv.fnal.gov on the Internet.

	D'_0	D'_0	D'_-	D'_-
Q_0^2[GeV^2]	4	10	4	10
λ_g	0.0	-0.146	-0.5	-0.489
γ_g	0.0	-0.146	10.6	5.74
A_g	2.78	2.04	0.338	0.466
η_g	5.3	5.43	5.3	5.56
η_1	0.42	0.421	0.42	0.422
η_2	3.92	4.04	3.92	4.03
ϵ_{ud}	2.31	2.20	2.59	2.43
γ_{ud}	4.43	2.98	4.21	2.74
A_{ud}	1.456	1.61	1.422	1.58
η_S	10.0	10.12	7.4	7.65
A_S	2.03	1.75	0.083	0.133
γ_S	8.47	8.28	15.8	10.2
ϵ_S	-2.98	-2.76	8.57	4.88
λ_S	0.0	-0.0711	-0.5	-0.489

Table 1: Distribution parameters at the starting value Q_0

dimension, Eq.(47). In all four approximations the value of the strong coupling α_s was taken to be 0.2644 at the starting value, $Q_0^2 = 4$ GeV^2, leading to the following couplings at M_Z,

$$\begin{aligned} \alpha_s(M_Z) &= 0.1171 \quad 1 \text{ loop, L} \\ \alpha_s(M_Z) &= 0.1123 \quad 2 \text{ loop, NL} \\ \alpha_s(M_Z) &= 0.1119 \quad 3 \text{ loop, NNL and NNNL} \end{aligned} \tag{58}$$

Fig. 1 shows the evolution of the singlet quark D'_0 distribution in these four approximations starting from $Q_0^2 = 4$ GeV^2. The heavy line shows the starting distribution in the following figures. We have checked that our numerical solution of the GLAP equation is close to the parameterization of MRS in the NL case, (as it should be!). The corrections to the singlet distribution Σ are substantial in the HERA region. This is because the NL approximation introduces $1/\omega$ terms, *cf.* Eq. (45) and the NNL approximation introduces $1/\omega^2$ terms. The NNL and NNNL curves are so close that they are hard to distinguish especially at $Q^2 = 10$ GeV^2.

Fig 2 shows the corresponding curves starting from the steeper D'_- distribution. The effect of the higher order terms is less significant because of the presence of a pole at $\omega = 1/2$ in the starting distribution. The effective value of ω is not very small. Note also that the x-dependence of Σ at small x is unchanged by the evolution. We will give an analytic understanding of these results in the next section. In this the NNL and NNNL curves overlap and cannot be distinguished on the plot.

Fig. 3 shows the curve for the gluon distribution starting from D'_0. The NL terms are much less significant and tend to decrease the growth of the gluon distribution, *cf.* Eqs. (43,45). The NNL terms are dependent on our assumption about the values of δ and η, *cf.* Eqs. (47). The NNNL terms become important at small x because of the $1/\omega^4$ pole. Fig. 4 shows the corresponding results for the steeper D'_- distribution. The influence of the higher order corrections is much smaller. The numerical influence of the unknown parameters δ and η can be tested by varying them. Fig. 5 shows Σ calculated in NNL order with two different assumptions about the value of δ and η. The result for Σ is relatively insensitive to these parameters. Their influence on the gluon distribution can be extracted by comparing the NL and NNL curves in Fig. 3.

We have also investigated how much the restriction to higher Q^2 will decrease the size of the higher order corrections. We have considered a starting value of $Q_0^2 = 10$ GeV^2. At such a starting value one is well into the deep inelastic region. In Figs. 6 and 7 we show evolution starting for $Q_0^2 = 10$ GeV^2. The starting distributions at $Q_0^2 = 10$ GeV^2 have been taken as the NL evolved shape of the D'_0 and D'_- distributions at this Q^2. The strong coupling, α_s was taken to be 0.2241 at the starting value, $Q_0^2 = 10$ GeV^2. The parameterization of the shape of these distributions is given in Table 1. The heavy line shows the starting distribution. The corrections to the D'_0 distribution at $Q^2 = 100$ GeV^2 are still quite large even in the restricted HERA range. Note that in the NL approximation the evolution back to $Q^2 = 4$ GeV^2 reproduces the original MRS starting distributions.

4 Analytic estimates

4.1 Solution at small ω

In this section we attempt to explain the main features of our numerical results using simple analytic estimates. In the small ω limit the eigenvalues of $\mathbf{P_0}$ are

$$\lambda_+ \approx \frac{2C_A}{\omega} + \lambda_c, \quad \lambda_- \approx -\frac{4C_F T_R f}{3C_A} \tag{59}$$

where

$$\lambda_c = -\frac{11C_A}{6} + \frac{2T_R f}{3}\Big(\frac{2C_F}{C_A} - 1\Big) \tag{60}$$

Note that λ_c is numerically significant. The accuracy of Eq. (59) in the relevant range of ω is illustrated in Fig. 8, which shows the exact value of $\lambda_\pm$ from Eq. (29) compared with the small ω expansion given by Eq. (59). One can see from Fig. 8 that $\lambda_+ \gg \lambda_-$ at small ω.

The projection operator $\mathbf{M}_+$, defined in Eq. (30) is given by,

$$\mathbf{M}_+ = \begin{pmatrix} 0 & 0 \\ \frac{C_F}{C_A} & 1 \end{pmatrix} + \omega\frac{2T_R f}{3C_A^2}\begin{pmatrix} C_F & C_A \\ \rho & -C_F \end{pmatrix} + O(\omega^2) \tag{61}$$

where $\rho = \frac{C_F C_A}{4T_R f} + \frac{C_F}{2} - \frac{2C_F^2}{C_A}$ and $\mathbf{M}_- = \mathbf{1} - \mathbf{M}_+$.

Since for small ω the eigenvalue λ_+ dominates, we may drop the λ_- term in Eq. (36) and reduce the problem to a single eigenvalue. Hence we can neglect the contribution of the $\mathbf{M}_-$ term in the general solution, Eq. (32). We will use this approximation in the following to simplify our analytic work. In lowest order this corresponds to writing

$$\mathbf{F}(\omega, t) \approx \mathbf{M}_+ \exp(\lambda_+ t)\mathbf{F}(\omega, 0) \tag{62}$$

As a result of the simplification of retaining only the dominant eigenvalue the two singlet GLAP equations are effectively reduced to one. The singlet quark distribution is expressible in terms of the gluon distribution. This is a general result and the relationship between Σ and G can be derived in terms of the anomalous dimension matrix.

If we further specialise to the limit defined by Eq. (38) we may write a simple formula for the relationship between Σ and G.

$$\begin{aligned}
\Sigma(\omega,Q^2) &= \frac{f}{9}\Big[1+\Big(\frac{f}{162}-\frac{1}{6}\Big)\omega+\Big(\frac{5\pi^2}{54}-\frac{1}{2}+\frac{97f}{1944}-\frac{7f^2}{26244}\Big)\omega^2 \\
&\quad +10\frac{a}{\omega}+a\Big(\pi^2-\frac{79}{6}+\frac{103f}{162}\Big)+56\frac{a^2}{\omega^2}+O(\epsilon^3)\Big]\omega G(\omega,Q^2) \qquad (63)\\
\frac{d\Sigma(\omega,Q^2)}{d\ln Q^2} &= \frac{2fa}{3}\Big[1-\frac{13}{12}\omega+\Big(\frac{109}{72}-\frac{2\pi^2}{27}\Big)\omega^2 \\
&\quad +10\frac{a}{\omega}+a\Big(\frac{40f}{81}+\pi^2-\frac{63}{2}\Big)+56\frac{a^2}{w^2}+O(\epsilon^3)\Big]G(\omega,Q^2) \qquad (64)
\end{aligned}$$

where ϵ is defined in the sense of Eq. (39). Eqs. (63,64) can be derived directly from the GLAP evolution equation assuming that G and Σ are proportional.

4.2 Analytic results at small x

The x behaviour of the distribution functions is obtained by performing the inverse Mellin transform. For simple starting distributions this can be evaluated analytically at small x. This exercise allows us to find the dominant values of ω in the integral and hence test the validity of Eq. (38). At small x the integrals we have to evaluate involve the starting distribution and simple powers of ω and are of the form,

$$\begin{aligned}
xf(x,t) &= \frac{1}{2\pi i}\int_C d\omega\; x^{-\omega}\exp\Big(\lambda_+(\omega)t\Big)f(\omega,0) \\
&\equiv \frac{1}{2\pi i}\int_C d\omega\; \exp\Big(\lambda_+(\omega)t+\omega y\Big)f(\omega,0) \qquad (65)
\end{aligned}$$

where $y=-\ln x$ and the contour is to the right of all singularities of the starting value in the ω representation, $f(\omega,0)$.

Eq. (65) allows us to investigate the influence of the initial condition on the behaviour of the structure function. Let us assume a simple starting distribution of the form.

$$xf(x,0)=Ax^{-\omega_0},\;\; f(\omega,0)=\frac{A}{\omega-\omega_0}. \qquad (66)$$

We now evaluate the integral Eq. (65) with the starting distribution in Eq. (66) in two different situations.

4.2.1 $\omega_0 < \omega_S$

In the first instance let us assume that ω_0 is less than the ω_S, the value at which the integrand has a saddle point. At large y and t the saddle point of the integrand in Eq. (65) is determined by the condition,

$$\frac{d}{d\omega}\{\omega y + \lambda_+(\omega)t\}\bigg|_{\omega=\omega_S} = 0 \tag{67}$$

In the limit $\omega \to 0$ the anomalous dimension λ_+ is given by Eq. (59) so that the saddle point value, ω_S is found to be,

$$\omega_S = \sqrt{\frac{\bar{t}}{y}}; \quad \bar{t} = 2C_A t \tag{68}$$

If $\omega_0 < \omega_S$ we can estimate the integral Eq. (65) using the method of steepest descent to give

$$xf(x) = \sqrt{\frac{\pi}{\omega_S^3 \bar{t}}} \exp\left(2\sqrt{y\bar{t}}\right) f(\omega_S, 0). \tag{69}$$

In the particular case that the initial distribution has a $1/x$ behaviour, $f(\omega, 0) = 1/\omega$ we can calculate all integrals exactly without recourse to the method of steepest descents. The modified Bessel function of the first kind has the integral representation[25]

$$I_n(2\sqrt{\bar{t}y}) = \frac{1}{2\pi i}\int_C \frac{d\omega}{\omega}\left(\frac{\omega_S}{\omega}\right)^n \exp\left(\frac{\bar{t}}{\omega} + y\omega\right). \tag{70}$$

This allows us to give an exact analytic evaluation of any integral involving a polynomial in ω, such as the expressions in Eq. (63,64). Let us define the average value of $1/\omega^n$.

$$\left\langle\frac{1}{\omega^n}\right\rangle = \int_C \frac{d\omega}{\omega}\frac{1}{\omega^n}\exp\left(\frac{\bar{t}}{\omega} + y\omega\right) \bigg/ \int_C \frac{d\omega}{\omega}\exp\left(\frac{\bar{t}}{\omega} + y\omega\right) \tag{71}$$

$$\left\langle\frac{1}{\omega^n}\right\rangle = \frac{1}{\omega_S^n}\frac{I_n(2\sqrt{\bar{t}y})}{I_0(2\sqrt{\bar{t}y})} \tag{72}$$

Eq. (72) holds for both positive and negative n, $(I_{-n}(z) \equiv I_n(z))$. Thus

$$\langle\omega\rangle = \omega_S \frac{I_{-1}(2\sqrt{\bar{t}y})}{I_0(2\sqrt{\bar{t}y})} \tag{73}$$

The asymptotic expansion of the modified Bessel functions for large z is[25]

$$I_n(z) = \frac{e^z}{\sqrt{2\pi z}}[1 - \frac{4n^2 - 1}{8z} + O(\frac{1}{z^2})] \tag{74}$$

so that

$$\langle\omega^n\rangle = \omega_S^n[1 - \frac{n^2}{2z} + O(\frac{1}{z^2})]. \tag{75}$$

Using the asymptotic expansion in Eq. (74) and retaining only the first term, gives the saddle point result, Eq. (69) for f, with the position of the saddle point given by Eq. (68). Eqs. (74,75) can be used to estimate the corrections to the saddle point result. We expect large corrections when $n^2 \sim 2\sqrt{\bar{t}y}$. Fig. 9 indicates the value of the saddle point ω_S in the HERA region with $Q_0 = 2$ GeV and $\Lambda = 230$ MeV. The heavy diagonal line shows the upper boundary of the HERA kinematic region. The saddle point value ω_S is only small for small evolutions and for small x.

So with a flat starting distribution we find that ω_S can be small enough that it makes sense only to retain the singular terms in the anomalous dimension. Unfortunately this also means that Eq. (38) is not satisfied and that we are beyond the critical value where finite order perturbation theory makes sense. We will discuss this breakdown of perturbation theory later.

4.2.2 $\omega_0 > \omega_S$

In this case the singularity in the initial condition becomes the rightmost singularity. As an example of this type of distribution, the D'_- parametrization of MRS[28] has $\omega_0 = 1/2$. If $\omega_0 = 1/2$ we see from Fig. 9 that the condition $\omega_0 > \omega_S$ holds in most of the HERA kinematical region for $x < 10^{-2}$. The singularity of the initial distribution at ω_0 and the essential singularity of the kernel at $\omega = 0$ do not coincide. The singularity in the initial distribution is the rightmost dominating singularity. Its contribution can easily be calculated by closing the contour around the pole at ω_0 and using the theorem of residues. Eq. (65) gives

$$xf(x,t) = A\exp(\lambda_c t)\Big[\exp(\frac{\bar{t}}{\omega_0} + y\omega_0) + \frac{1}{2\pi i}\int_{C'} d\omega \frac{1}{\omega - \omega_0}\exp\big(\frac{\bar{t}}{\omega} + \omega y\big)\Big] \quad (76)$$

The contour C' is to left of ω_0. The second integral can be evaluated approximately for $\omega_S < \omega_0$. The result is

$$xf(x,t) = A\exp(\lambda_c t)\Big[\exp(\frac{\bar{t}}{\omega_0} + y\omega_0) - \frac{\omega_S}{\omega_0} I_1(2\sqrt{\bar{t}y}) + O(\frac{\omega_S^2}{\omega_0^2})\Big]. \quad (77)$$

By examination of the exponents one sees that pole term always dominates. Indeed, the ratio R of the second term to the first is equal to

$$R = -\frac{\omega_S}{\omega_0}\frac{1}{\sqrt{4\pi\omega_S y}}\exp\Big[-\omega_0 y\Big(1 - \frac{\omega_S}{\omega_0}\Big)^2\Big] \quad (78)$$

R is small for $\omega_0 = 0.5$ and $x < 10^{-2}$. As a result of the neglect of the second term the inverse Mellin transform is dramatically simplified. We only need the anomalous dimension at the pole value $\omega = \omega_0$ fixed by the starting distribution! We will exploit this simplification in section 5. Preliminary indications from data are that the case $\omega_0 \sim \frac{1}{2}$ holds experimentally.

4.3 Validity of our approach

The following limit on the value of ω defines the region of validity of our approach,

$$\omega_L \sim \alpha_s(Q_0^2) \le \sqrt{\alpha_s(Q_0^2)} \le \omega \ll 1. \quad (79)$$

Only for values of ω which satisfy Eq. (79) can we trust our calculation of the kernels in the GLAP equation. The purpose of this subsection is to give numerical estimates of the values of ω and x for which we can apply our method.

We shall now estimate the value of ω_L. We shall take as our defining equation for ω_L the condition that the GG component of the anomalous dimension matrix, (which we denote by γ), equals $\frac{1}{2}$.

$$\gamma(\omega_L) \equiv P_{GG}(\omega_L) = \frac{1}{2} \quad (80)$$

Eq. (80) is an exact result of the BFKL equation, which sums only the leading $1/\omega$ singularities. We propose to use Eq. (80) as a limitation on the anomalous dimension in more general circumstances.

Let us first review the status of Eq. (80) in the BFKL equation. In the solution of the BFKL equation the anomalous dimension γ is defined implicitly by the equation,

$$\begin{aligned} 1 &= \frac{\alpha_s C_A}{\pi\omega}\chi(\gamma) && (81) \\ \chi(\gamma) &= 2\psi(1) - \psi(\gamma) - \psi(1-\gamma) && (82) \end{aligned}$$

where the function $\psi(z) = \Gamma'(z)/\Gamma(z)$. The function χ has a minimum at the symmetry point $\gamma = 1/2$. Around the symmetry point we have

$$\chi(\gamma) \rightarrow 4\ln 2 + 14\zeta(3)(\gamma - \frac{1}{2})^2 + \ldots \tag{83}$$

This leads to the result

$$\omega_L^0 = \frac{4C_A\alpha_s \ln 2}{\pi} \tag{84}$$

The symmetry which gives the point $\gamma = \frac{1}{2}$ a special status is the scale invariance of the theory. To illustrate this result let us consider the cross section for the interaction of two spacelike virtual photons with virtualities Q^2 and Q_0^2. In the case $Q^2 \gg Q_0^2$ the moments of the cross section can be written in the form

$$M(Q^2, Q_0^2; \omega) = \frac{1}{Q^2}\exp\Big(\frac{\gamma(\omega)}{b_0 a(Q^2)}\ln\frac{a(Q_0^2)}{a(Q^2)}\Big) \tag{85}$$

while for $Q_0^2 \gg Q^2$ we have

$$M(Q^2, Q_0^2; \omega) = \frac{1}{Q_0^2}\exp\Big(\frac{\gamma(\omega)}{b_0 a(Q_0^2)}\ln\frac{a(Q^2)}{a(Q_0^2)}\Big). \tag{86}$$

The observation of BFKL was the fact that the matching between the two kinematic regions shown above should occur not only at $Q^2 = Q_0^2$ but also in the whole region $Q^2 \sim Q_0^2$. In this region

$$\frac{1}{b_0}\ln\frac{\alpha_s(Q_0^2)}{\alpha_s(Q^2)} \rightarrow a(Q_0^2)\ln\frac{Q^2}{Q_0^2} \tag{87}$$

So matching the functions in front of $\ln Q^2/Q_0^2$ one obtains the relation,

$$1 - \gamma(\omega) = \gamma(\omega) \tag{88}$$

which is equivalent to Eq. (80). The above argument depends only on the scale invariance of the theory and does not depend on the accuracy of our calculation for the anomalous dimension. To the extent that we can ignore scale breaking effects such as the running of the coupling it should be correct in any order of perturbative QCD. This is the reason why we want to use Eq.(80) to calculate the value of ω_L for the perturbative anomalous dimension as defined in section 2.3.

Fig. 10 shows the GG element of the anomalous dimension in various approximations. The GG component of the anomalous dimension has a perturbative expansion.

$$\gamma(\omega) = aP_0^{GG} + a^2 P_1^{GG} + a^3 P_2^{GG} + a^4 P_3^{GG} + \ldots \tag{89}$$

The curves shown are the cumulative sum through to the specified order of perturbation theory. The L and NL terms are included exactly. The NNL terms are from the GG element of Eq. (47) with $\eta = 1$ and the NNNL term from Eq. (48). We have chosen the running coupling $\alpha_s = 0.2241$ which is the value appropriate for $Q^2 = 10$ GeV^2 with our choice of Λ. Also shown in Fig. 10 (marked as BFKL) is the value of γ obtained from a solution of Eq. (81).

This BFKL curve does a poor job of approximating the perturbative anomalous dimension. We have tried to estimate the corrections to this curve by imposing momentum conservation on the kernel of the BFKL equation. We replace $1/\omega$ in Eq. (81) by $1/\omega - 1$. This implements momentum conservation in the BFKL equation since the kernel of the equation now vanishes for $\omega = 1$. We cannot prove that is the correct answer but this procedure works quite well for the leading order anomalous dimension and we hope that it give a correct estimate of the scale of possible next order corrections to the BFKL equation. The result for the anomalous dimension after such a substitution is shown in Fig.10 marked as BFKL$'$. The BFKL$'$ curve matches the perturbative anomalous dimension much more closely. The value of ω_L' obtained from this modification of Eq. (81) is

$$\omega_L' = \frac{\omega_L^0}{1 + \omega_L^0}. \tag{90}$$

In the example shown in Fig. 10 we see that the value of ω_L' is equal to 0.37 which is smaller than $\omega_L^0 \approx 0.60$ that we get from leading order calculations.

In summary we conclude from Eq. (79) and Fig. 10 that we can apply our approach only for $\omega > \omega_L = 0.35$. This means that if ω_0 is smaller than $\omega_L = 0.35$ (the case of a flat initial distribution) we can trust our solution only for $\omega_S > 0.35$. This corresponds to $x > 10^{-3}$ as can be seen from Fig. 9. In the case $\omega_0 > \omega_L = 0.35$ (the case of a steep initial distribution) we have no restriction on the values of x and Q^2 for applicability of our approach.

The reduction of the solution to the GLAP evolution equation to a one dimensional problem taking the pole $\omega = \omega_0$ in integral Eq. (65) is a separate issue. To justify this simplification we need

$$\omega_0 > \omega_S. \tag{91}$$

From Fig. 9 we conclude that such an approach is valid only for $x < 10^{-2}$ in the HERA kinematic region if $\omega_0 = \frac{1}{2}$.

5 Deep inelastic structure functions at small x

We shall consider only the deep inelastic structure function F_2 which is given in terms of parton densities as

$$\begin{aligned} F_2(x,Q^2) &= x\int_x^1 \frac{dz}{z}\Big\{ \left\langle e^2 \right\rangle \left[C^{FF}(z,Q^2)\Sigma(\frac{x}{z},Q^2) + C^{FG}(x,Q^2)G(\frac{x}{z},Q^2)\right] \\ &+ \frac{1}{6}C^{NS}(z,Q^2)\Delta_{NS}(\frac{x}{z},Q^2)\Big\} \end{aligned} \tag{92}$$

with

$$\left\langle e^2 \right\rangle = \frac{4f_u + f_d}{9f}, \quad f = f_u + f_d, \tag{93}$$

where C denotes the coefficient functions, f_u and f_d denote the number of quarks with $Q = \frac{2}{3}$ and $Q = -\frac{1}{3}$, and the non-singlet parton density Δ_{NS} is given in terms of the non-singlet combinations defined in Eqs. (14,15).

$$\Delta_{NS} = T_3 + \frac{1}{3}(T_8 - T_{15}) + \frac{1}{5}(T_{24} - T_{35}) \equiv \frac{2f_d}{f}\sum_{i=1}^{f_u} q^+_{u,i} - \frac{2f_u}{f}\sum_{i=1}^{f_d} q^+_{d,i} \tag{94}$$

For an even number of flavors $\langle e^2 \rangle = 5/18$ and $\Delta_{NS} = \sum_{i=1}^{f/2}(q^+_{u,i} - q^+_{d,i})$.

Figs. 11-14 show the predictions for F_2 in leading (L), next-to-leading (NL) and next-to-next-to leading (NNL) order in the HERA range at four different values of Q^2 corresponding to the recent Zeus and H1 measurement of F_2. The lower and upper sets of curves correspond to the MRS D_0' and MRS D_-' initial distributions evolved from $Q_0^2 = 4$ GeV^2. Also shown are the recently published data of the H1 and Zeus collaborations[7,8] together with the systematic and statistical errors. The experimental errors are still large; the data are included on the plots to indicate in a concrete way the range that can be covered by experiments at HERA. A starting distribution steeper than $1/x$ appears to be favoured by the data.

6 Estimate of the gluon distribution function from F_2

6.1 Description of the method

Using our analytic results we can also estimate the gluon distribution directly from the measurement of the $F_2(x, Q^2)$ structure function at HERA. In this subsection we will describe the method, using the lowest order formula as an illustration. The basic idea is that the Q^2 derivative of F_2 is sensitive to the gluon distribution function[29]. Let us first define the quantity $\overline{\Sigma}$ from the experimental data for F_2

$$\overline{\Sigma}(x, Q^2) = \frac{F_2(x, Q^2)}{x \langle e^2 \rangle}. \tag{95}$$

Knowledge of $\overline{\Sigma}$ as a function of x and Q^2 is the input which we obtain from experiment. For four active flavours $\langle e^2 \rangle = 5/18$. From Eq. (92) we have to lowest order in α_s that

$$F_2(x, Q^2) = x \left\langle e^2 \right\rangle \Sigma(x, Q^2) \tag{96}$$

where we have ignored the non-singlet contribution which gives a small contribution at small x. Therefore in lowest order and at small x we can identify Σ and $\overline{\Sigma}$.

The lowest order GLAP equation for Σ reads

$$\frac{d\Sigma(x, Q^2)}{d \ln Q^2} = \frac{\alpha_s}{2\pi} \int_x^1 \frac{dz}{z} \left[P_0^{FF}(z) \Sigma(\frac{x}{z}) + P_0^{FG}(z) G(\frac{x}{z}) \right]. \tag{97}$$

The information about the gluon is difficult to extract from this equation at normal x because it involves a weighted integral over the quark and gluon distribution functions. In moment space this means that we have to know the moments of Σ and $d\Sigma/d\ln Q^2$ at all values of ω. Taking moments of Eq. (97) we have that

$$\frac{d\Sigma(\omega)}{d\ln Q^2} = \frac{\alpha_s}{2\pi}\left[P_0^{FF}(\omega)\Sigma(\omega) + P_0^{FG}(\omega)G(\omega)\right]. \tag{98}$$

If ω were known to be very small we could neglect P_0^{FF} term in lowest order because $P_0^{FF}(0) = 0$. However the dominant value of ω is unlikely to be that small and furthermore this simplification does not occur in higher orders. We therefore retain the term proportional to Σ in Eq. (98).

Let us assume a simple form for the gluon distribution,

$$xG(x) = A_g x^{-\omega_0}, \quad x\Sigma(x) = A_\Sigma x^{-\omega_0} \tag{99}$$

where $\omega_0 > 0$. Taking moments we have

$$G(\omega) = \frac{A_g}{\omega - \omega_0}, \quad \Sigma(\omega) = \frac{A_\Sigma}{\omega - \omega_0} \tag{100}$$

If in performing the inverse Mellin transform we find that ω_0 is to the right of the saddle point, ω_S, only a single value of ω contributes as discussed in Section 4. Eq. (98) assumes the simple form,

$$\frac{d\Sigma(\omega)}{d\ln Q^2} = \frac{\alpha_s}{2\pi}\left[P_0^{FF}(\omega_0)\Sigma(\omega) + P_0^{FG}(\omega_0)G(\omega)\right]. \tag{101}$$

The value of ω_0 can be determined by the measured slope of F_2.

$$\omega_0 = \frac{d\ln\overline{\Sigma}}{d\ln(1/x)} \tag{102}$$

We therefore find that

$$\frac{d\overline{\Sigma}(x,Q^2)}{d\ln Q^2} = \frac{\alpha_s}{2\pi}\left[P_0^{FF}(\omega_0)\overline{\Sigma}(x,Q^2) + P_0^{FG}(\omega_0)G(x,Q^2)\right] \tag{103}$$

Since the GLAP kernels are known as a function of ω, G can be determined.

ω	p_0^{FF}	p_1^{FF}	p_2^{FF}	p_0^{FG}	p_1^{FG}	p_2^{FG}
.1	-0.04079	2.812	36.81	.3832	6.521	81.23
.2	-0.07729	.9977	8.622	.3497	2.512	18.70
.3	-.1104	.4453	3.586	.3220	1.345	7.652
.4	-.1406	.1909	1.877	.2987	.8471	3.944
.5	-.1685	0.04707	1.109	.2789	.5976	2.298
.6	-.1944	-0.04609	.7023	.2619	.4610	1.441
.7	-.2186	-.1129	.4631	.2470	.3824	.9458
.8	-.2413	-.1647	.3114	.2340	.3360	.6390
.9	-.2627	-.2075	.2095	.2225	.3086	.4385
1.	-.2829	-.2444	.1381	.2122	.2929	.3019

Table 2: Coefficients required to obtain gluon distribution.

The extension of the basic result to include higher orders is straightforward but tedious. The details of the derivation are given in the next subsection. The full result is of the form

$$\frac{d\overline{\Sigma}(x,Q^2)}{d\ln Q^2} = \mathcal{P}^{FF}(\omega_0)\overline{\Sigma}(x,Q^2) + \mathcal{P}^{FG}(\omega_0)G(x,Q^2) \tag{104}$$

with ω_0 given by Eq. (102) and $\overline{\Sigma}$ given by Eq. (95). Eq. (104) is the basis of our method for determining G. With our definitions of $\mathcal{P}$ the measured gluon distribution G is in the $\overline{MS}$ scheme. The functions $\mathcal{P}$ have perturbative expansions.

$$\mathcal{P}^{FF}(\omega) = \alpha_s p_0^{FF} + \alpha_s^2 p_1^{FF} + \alpha_s^3 p_2^{FF} + O(\alpha_s^4) \tag{105}$$

$$\mathcal{P}^{FG}(\omega) = \alpha_s p_0^{FG} + \alpha_s^2 p_1^{FG} + \alpha_s^3 p_2^{FG} + O(\alpha_s^4) \tag{106}$$

We may tabulate contributions to $\mathcal{P}^{FF}, \mathcal{P}^{FG}$ for plausible values of ω and hence obtain the result for the gluon distribution. Table 2 gives the coefficients in the expansion for various ω.

Thus, for example taking $\omega_0 = 0.5$ and $\alpha_s = 0.2241$, (the value appropriate for $Q^2 = 10$ GeV^2) we obtain keeping all terms up to α_s^3.

$$G(x,Q^2) = 8.45\frac{d\overline{\Sigma}(x,Q^2)}{d\ln Q^2} + 0.194\overline{\Sigma}(x,Q^2) \tag{107}$$

The term proportional to $\overline{\Sigma}$ in Eq. (107) is not entirely negligible. This means that attempts to get the value of $G(x, Q^2)$ dropping this term are somewhat misleading[29]. There are also large changes between different orders in the perturbation theory. In fact in leading order the equivalent relation to Eq.(107) is

$$G(x, Q^2) = 16.0 \frac{d\overline{\Sigma}(x, Q^2)}{d \ln Q^2} + 0.604 \overline{\Sigma}(x, Q^2) \tag{108}$$

Examination of the different coefficients $\mathcal{P}^{FF}, \mathcal{P}^{FG}$ given in Table 2 shows that the accuracy of the extraction of the value of $G(x, Q^2)$ from Eq. (104) cannot be very good. In fact for $\omega_0 = 0.5$ we estimate the theoretical error on the gluon distribution to be about 20%. The advantage of the method is that it allows us to extract the gluon distribution directly from the experimental observables,

$$\overline{\Sigma}(x, Q^2), \ \frac{d \ln \overline{\Sigma}(x, Q^2)}{d \ln x}, \ \frac{d\overline{\Sigma}(x, Q^2)}{d \ln Q^2} \tag{109}$$

Our achievement is rather modest since we have assumed the $x^{-\omega_0}$ behaviour of initial structure function and only claim to determine the normalization constant in front. In addition the method requires knowledge of the strong coupling constant, α_s. However since it gives a simple way to estimate the gluon distribution directly from F_2 it may be of interest to the experimental community.

6.2 Technical details of our method

The moment of the singlet part of F_2 with overall factors removed is defined as $\overline{\Sigma}(\omega)$. In the $\overline{MS}$ scheme $\overline{\Sigma}$ is given by,

$$\overline{\Sigma}(\omega) = \mathbf{S}^T \mathbf{C}(\omega) \mathbf{F}(\omega) \tag{110}$$

where $\mathbf{S}$ is a projection operator onto the quark components

$$\mathbf{S} = \begin{pmatrix} 1 \\ 0 \end{pmatrix} \tag{111}$$

and $\mathbf{C}$ is the matrix of coefficient functions. $\mathbf{C}$ can be expanded in a power series in a

$$\mathbf{C} = \mathbf{1} + a\mathbf{C}_1 + a^2\mathbf{C}_2 + a^3\mathbf{C}_3 + \ldots \tag{112}$$

Thus for example the first order contribution to $\mathbf{C}$ may be written,

$$\mathbf{C}_1 = \begin{pmatrix} C_1^{FF} & C_1^{FG} \\ C_1^{GF} & C_1^{GG} \end{pmatrix} \tag{113}$$

The derivative of $\overline{\Sigma}$ with respect to Q^2 is given by

$$\frac{d\overline{\Sigma}}{d\ln Q^2} = \mathbf{S}^T \frac{d\mathbf{C}}{d\ln Q^2}\mathbf{F} + \mathbf{S}^T\mathbf{C}\frac{d\mathbf{F}}{d\ln Q^2} \tag{114}$$

We can use the GLAP equation to eliminate the Q^2 derivative in the second term and use Eq.(110) to eliminate Σ in favour of $\overline{\Sigma}$ and G, the gluon distribution in the $\overline{MS}$ bar scheme. The resultant equation is of the form,

$$\frac{d\overline{\Sigma}(\omega)}{d\ln Q^2} = \mathcal{P}^{FF}(\omega)\overline{\Sigma}(\omega) + \mathcal{P}^{FG}(\omega)G(\omega) \tag{115}$$

where

$$\begin{aligned}
\mathcal{P}^{FF} &= aP_0^{FF} + a^2(P_1^{FF} + C_1^{FG}P_0^{GF} - b_0C_1^{FF}) \\
&\quad + a^3(P_2^{FF} - C_1^{FF}C_1^{FG}P_0^{GF} + C_2^{FG}P_0^{GF} \\
&\quad + C_1^{FG}P_1^{GF} + b_0C_1^{FF}C_1^{FF} - 2b_0C_2^{FF} - b_1C_1^{FF}) \\
\mathcal{P}^{FG} &= aP_0^{FG} + a^2(P_1^{FG} + C_1^{FF}P_0^{FG} - P_0^{FF}C_1^{FG} + C_1^{FG}P_0^{GG} - C_1^{FG}b_0) \\
&\quad + a^3(P_2^{FG} + C_1^{FF}P_1^{FG} - P_1^{FF}C_1^{FG} + C_2^{FF}P_0^{FG} - P_0^{FF}C_2^{FG} + C_1^{FG}P_1^{GG} \\
&\quad + C_2^{FG}P_0^{GG} - C_1^{FG}P_0^{GF}C_1^{FG} + b_0C_1^{FF}C_1^{FG} - 2b_0C_2^{FG} - b_1C_1^{FG})
\end{aligned} \tag{116}$$

Note that in our approximation, Eq.(38) we get no contribution in order a^4. The $\overline{MS}$ coefficient functions are [26,27,30],

$$\begin{aligned}
C_1^{FF} &= C_F\left[(S_1(\omega) + \frac{3}{2} + \frac{1}{\omega+1} + \frac{1}{\omega+2})S_1(\omega) - S_2(\omega) - \frac{\omega(9\omega+17)}{2(\omega+1)(\omega+2)}\right] \\
C_1^{FG} &= 2T_Rf\left[\frac{2-\omega}{(\omega+2)(\omega+3)} - \frac{\omega^2+3\omega+4}{(\omega+1)(\omega+2)(\omega+3)}S_1(\omega)\right] \\
C_2^{FF} &= \frac{T_RfC_F}{2\omega}\Big(\frac{344}{27} - \frac{16}{3}\zeta(2)\Big) + O(1) \\
C_2^{FG} &= \frac{T_RfC_A}{2\omega}\Big(\frac{344}{27} - \frac{16}{3}\zeta(2)\Big) + O(1)
\end{aligned} \tag{117}$$

where S_1 and S_2 are expressable in terms of the first and second derivatives of the logarithm of gamma function[25].

$$S_1(\omega) = \psi(\omega+1) - \psi(1),\ S_2(\omega) = \psi'(1) - \psi'(\omega+1) \tag{118}$$

Since the full C_2^{FF} and C_2^{FG} are known[30] it would be interesting to evaluate Eq. (116) using the full expression. In our numerical work we have used the form given in Eq. (117) and the form for $\mathbf{P_2}$ given in Eq. (47).

7 Conclusions.

We have considered the solution to the GLAP equation in the space of moments. We hope that we have convinced the reader that the evolution of parton distributions using the moment space method is a numerically efficient technique. To evaluate a parton distribution at any value of Q^2 requires only a single integral in the complex ω plane. The small price one pays for this efficiency is the need to know the value of the starting distributions at all values of x, in order to construct the moments.

An additional benefit is that the moment space technique gives analytic insight into the structure of the solution. This is most helpful in understanding the numerical results and assessing their limitations. We find that the result of the evolution to the small x region depends on the relative magnitudes of ω_0, the exponent in the starting distribution and ω_S the saddle point of the inverse Mellin transform. This evolution using perturbative anomalous dimensions will be reliable only when the effective value of ω is larger than the critical value of ω_L.

One of the most interesting results revealed by the analytic and numerical work is that the growth with x of the parton distributions is determined by the starting value ω_0, if $\omega_0 > \omega_S$. We have exploited this simplification in our proposal to estimate the gluon distribution from F_2.

We are now in a position to answer the questions which we asked in the introduction. We see that the importance of the $\omega = 0$ singularities in the perturbative anomalous dimensions depends on the form of the initial distribution. If $\omega_0 > \omega_S$ the $\omega = 0$ singularities are never dominant, because ω is pinned down at ω_0. On the other hand if ω_0 is small, then we can have $1 \gg \omega_S > \omega_0$ and the anomalous dimensions are dominated by the $\omega = 0$ singularities.

We also have attempted to find out when the anomalous dimension is well represented by a finite number of terms of its expansion in powers of α_s. We have introduced a critical anomalous dimension and a corresponding critical value of ω which we denote by ω_L. When the effective value of ω is larger than ω_L the anomalous dimension is well represented by its perturbative expansion in α_s. We have attempted to estimate a more reliable value of ω_L than is provided by the BFKL equation.

The interpolation of data in the HERA range using the GLAP equation is only possible if $\omega > \omega_L$. Examination of Fig. 9 shows that the evolution of a flat starting distribution does not make sense in the HERA range below $x = 10^{-3}$. Thus for example the evolution of D_0' distribution is not reliably extrapolated below 10^{-3} using the GLAP equation. For a steeper distribution the GLAP equation is adequate as long as $\omega_0 > \omega_L$. However if $\omega_0 = \omega_L$ the GLAP equation cannot be used to interpolate the data at HERA, because the anomalous dimension is no longer perturbative.

We have found that the range of validity of the GLAP equation is severely curtailed at small x. This underscores the importance of finding a unified treatment of both logarithms of x and logarithms of Q^2.

Acknowledgements

One of us (RKE) would like to thank J. Forshaw, P. Nason and R. Roberts for helpful comments. We are grateful to the authors of ref.[30] for sending us their numerical program to calculate F_2. RKE would also like to thank ETH in Zurich, Switzerland and RAL in Didcot, UK for their hospitality. EML thanks the Fermilab Theory Group for hospitality extended to him.

References

1) L.V. Gribov, E.M Levin and M.G. Ryskin, *Phys. Rep.* **100** (1982) 1.

2) A.J. Askew *et al.*, Durham preprint, DTP-93-28, Sep 1993 ;
A.J. Askew *et al.*, *Phys. Rev.* **D47** (1993) 3775;
J. Kwiecinski *et al.*, *Phys. Rev.* **D44** (1991) 2640;
J. Kwiecinski *et al.*, *Phys. Rev.* **D42** (1990) 3645.

3) J. Kwiecinski, *Zeit. Phys.* **C29** (1985) 561.

4) L.N. Lipatov, in "Perturbative QCD", A. H. Mueller, (editor), (World Scientific, Singapore, 1989);

L.N. Lipatov and G.V. Frolov, *Sov. J. Nucl. Phys.* **13** (1971) 333;
E.A. Kuraev, L.N. Lipatov and V.S. Fadin, *Sov. Phys. JETP* **44** (1976) 443, *ibid.* **45** (1977) 199;
Ya.Ya. Balitskii and L.N. Lipatov, *Sov. J. Nucl. Phys.* **28** (1978) 822.

5) E.M. Levin et al., *Nucl. Phys.* **B357** (1991) 167.

6) E.M. Levin, Orsay lectures, LPTHE-91/02, (1991);
M. Krawczyk, Proceedings of the Desy Topical Meeting on Small x behaviour of Deep Inelastic Structure Functions, Hamburg (1990), A. Ali and J. Bartels, (Eds.), *Nucl. Phys.* B (Proc. Suppl.) 18C (1990) 64.

7) I. Abt et al., Desy Preprint DESY 93-117 (August 1993).

8) J. Martin, Proceedings of the XVI Symposium on Lepton-Photon Interactions, Cornell University, Ithaca, NY (August 1993).

9) J. Feltesse, Proceedings of the workshop on Physics at Hera, Hamburg, 1987, R. D. Peccei, (editor).

10) M. Klein, Proceedings of the workshop on Physics at Hera, Vol 1 Hamburg, 1991, W. Buchmüller and G. Ingelman (eds.).

11) G. Altarelli and G. Parisi, *Nucl. Phys.* **B126** (1977) 298;
Yu. L. Dokshitzer *Sov. Phys. JETP* **46** (1977) 641;
cf. L. N. Lipatov, *Sov. J. Nucl. Phys.* **20** (1975) 95;
V.N. Gribov and L.N. Lipatov, *Sov. J. Nucl. Phys.* **15** (1972) 438.

12) H. Georgi and H.D. Politzer, *Phys. Rev.* **D9** (1974) 416.

13) D. Gross and F. Wilczek, *Phys. Rev.* **D9** (1974) 980.

14) W-K Tung, *Nucl. Phys.* **B315** (1989) 378.

15) D.W.Mckay and J.P. Ralston, Proceedings of the Desy Topical Meeting on Small x behaviour of Deep Inelastic Structure Functions, Hamburg (1990), A. Ali and J. Bartels, (Eds.), *Nucl. Phys.* B (Proc. Suppl.) 18C (1990) 64.

16) S. Catani and F. Hautmann, *Phys. Lett.* **315B** (1993) 157.

17) I. Hinchliffe and C. H. Llewellyn Smith, *Nucl. Phys.* **B128** (1977) 93.

18) M. Diemoz et al, *Zeit. Phys.* **C39** (1988) 21.

19) O.V. Tarasov et al., *Phys. Lett.* **93B** (1980) 429.

20) G. Altarelli, *Phys. Rep.* **81** (1982) 1.

21) W. Furmanski and R. Petronzio, *Zeit. Phys.* **C11** (1982) 293.

22) E.G. Floratos et al., *Nucl. Phys.* **B192** (1981) 417.

23) W. Furmanski and R. Petronzio, *Phys. Lett.* **97B** (1980) 437.

24) T. Jaroszewicz, *Phys. Lett.* **116B** (1982) 291.

25) Handbook of Mathematical Functions, (eds. Abramowitz and Stegun) Dover, New York, 1965.

26) W.A. Bardeen *et al.*, *Phys. Rev.* **D18** (1978) 3998

27) G. Altarelli, R.K. Ellis and G. Martinelli, *Nucl. Phys.* **B157** (1979) 461

28) A. Martin, R. Roberts and W.J. Stirling, *Phys. Rev.* **D47** (1993) 867; *Phys. Lett.* **B306** (1993) 145, erratum, *Phys. Lett.* **B309** (1993) 492.

29) K. Prytz, *Phys. Lett.* **B311** (1993) 286.

30) W.L. van Neerven and E.B. Zijlstra, *Phys. Lett.* **B272** (1991) 127; *Nucl. Phys.* **B383** (1992) 525.

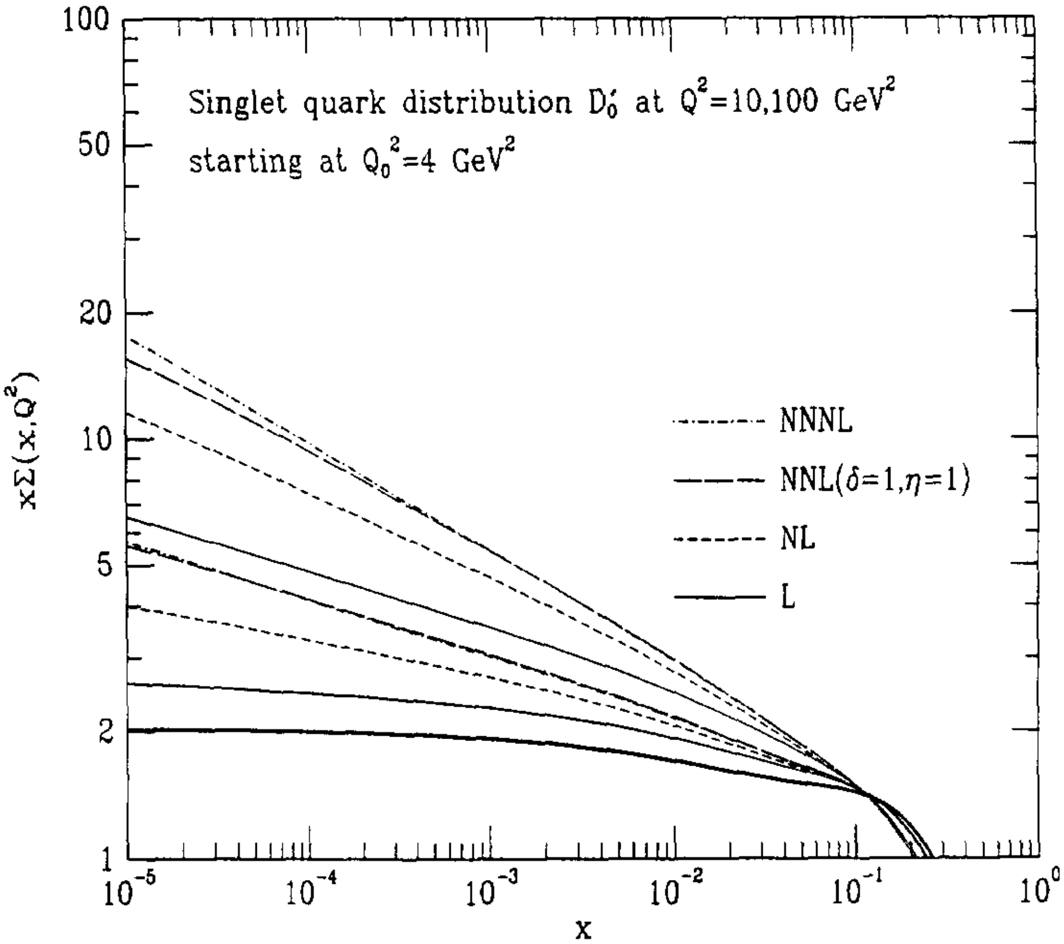

Figure 1: Evolution of D_0' quark singlet

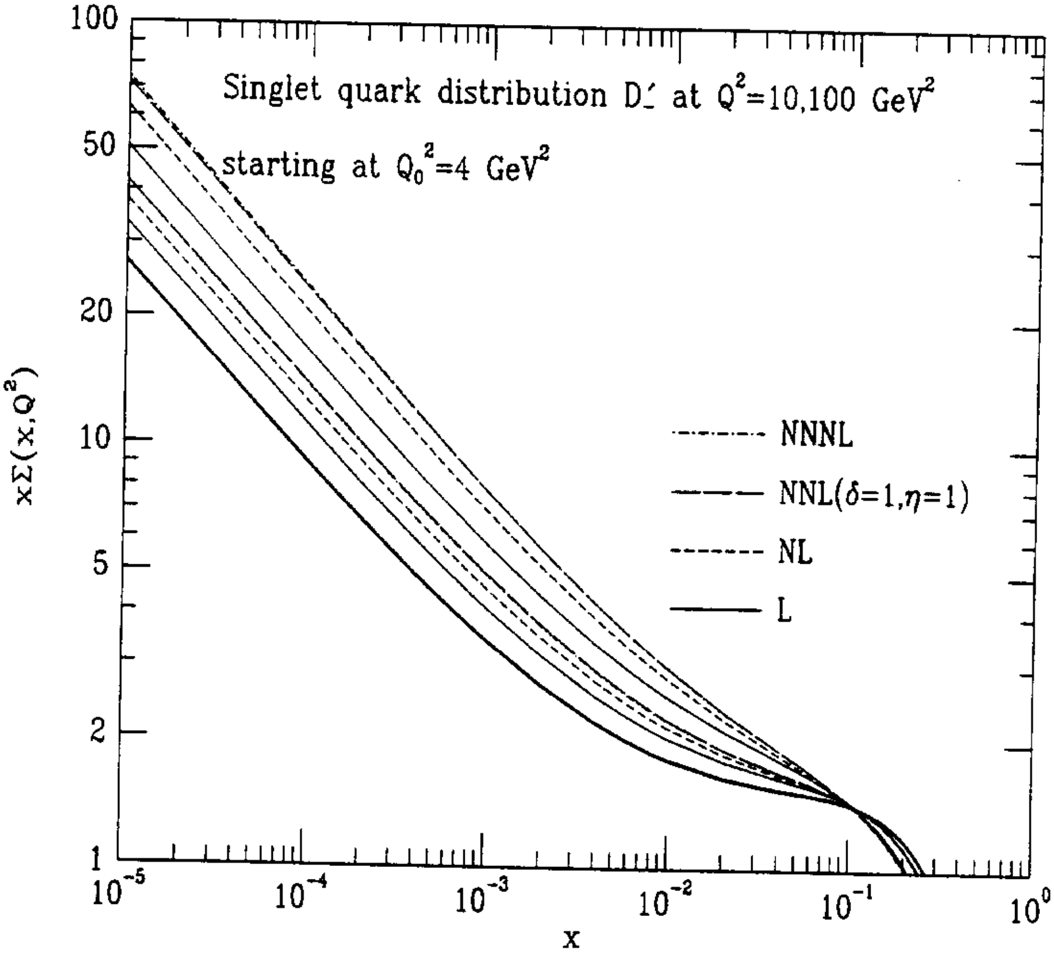

Figure 2: Evolution of D'_- quark singlet

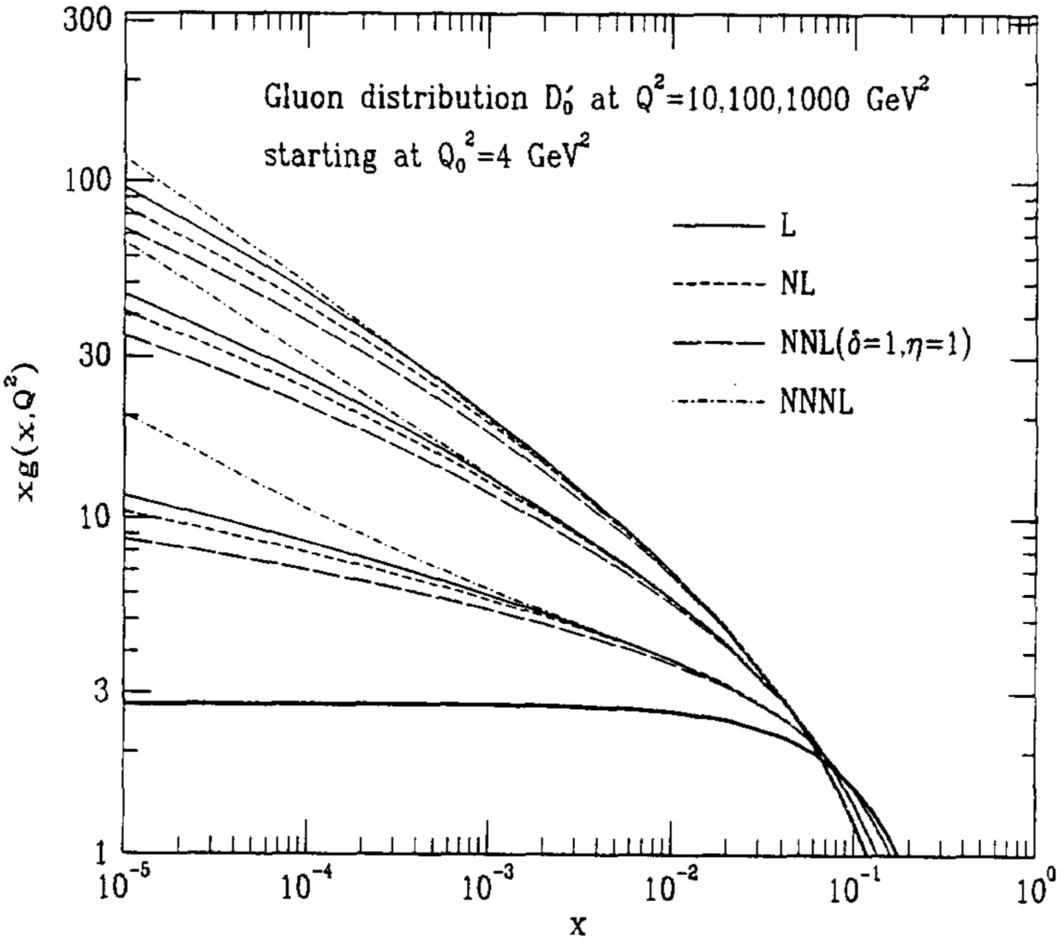

Figure 3: Evolution of D_0' gluon distribution

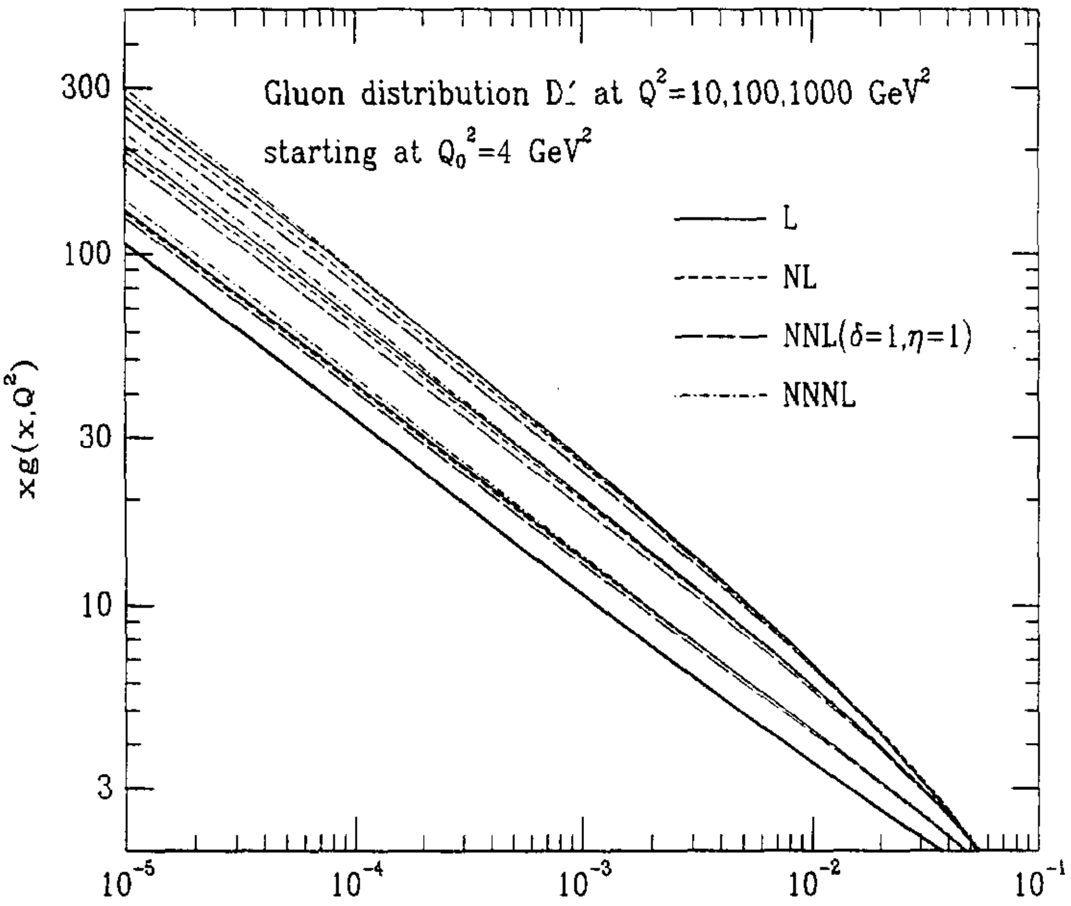

Figure 4: Evolution of D'_- gluon distribution

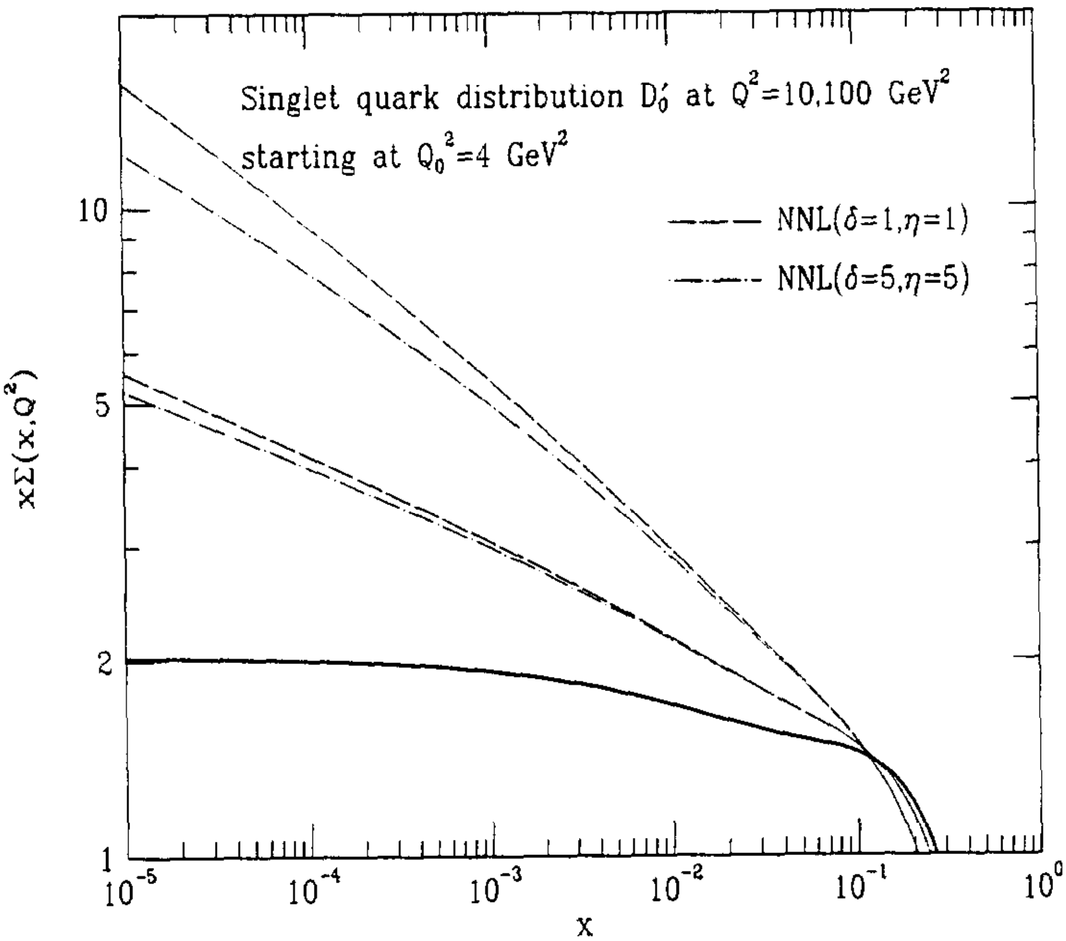

Figure 5: Evolution of D_0' singlet quark distribution with differing δ, η

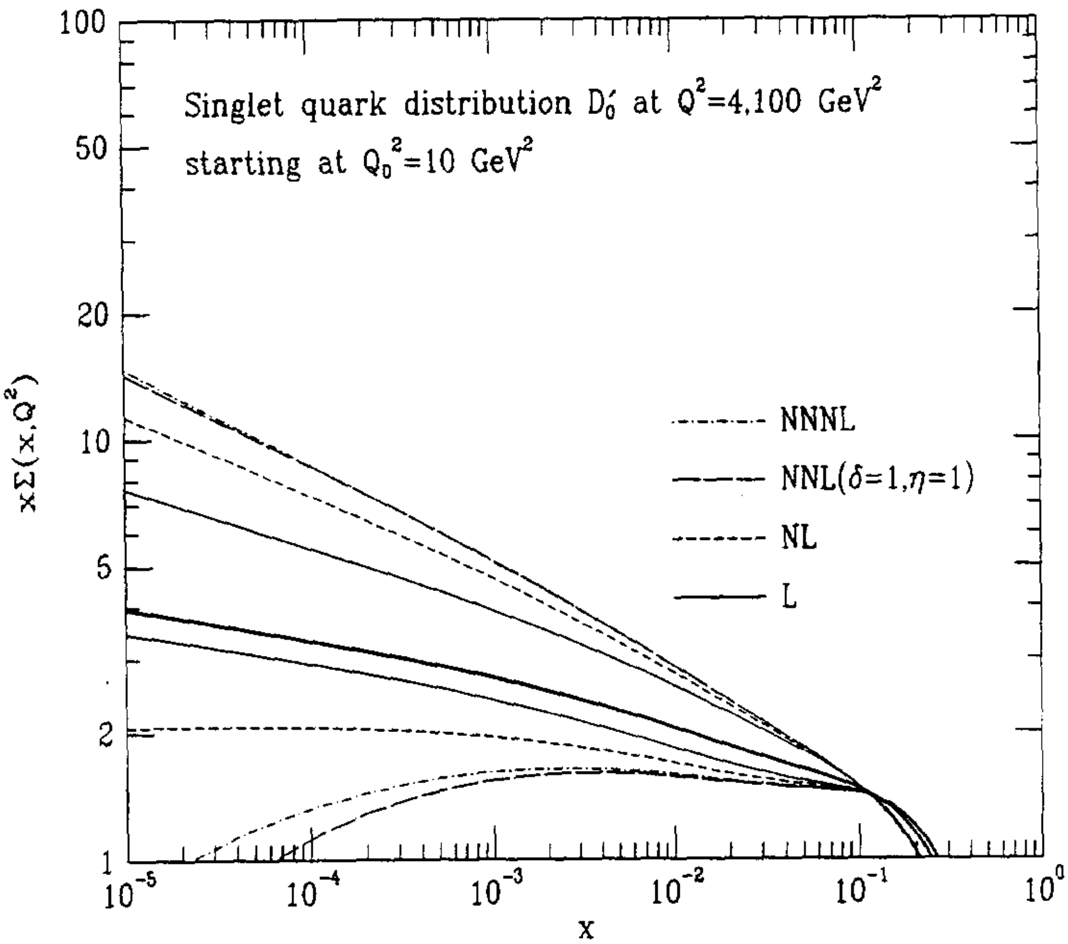

Figure 6: Evolution of D_0' gluon starting from $Q_0^2 = 10$ GeV^2

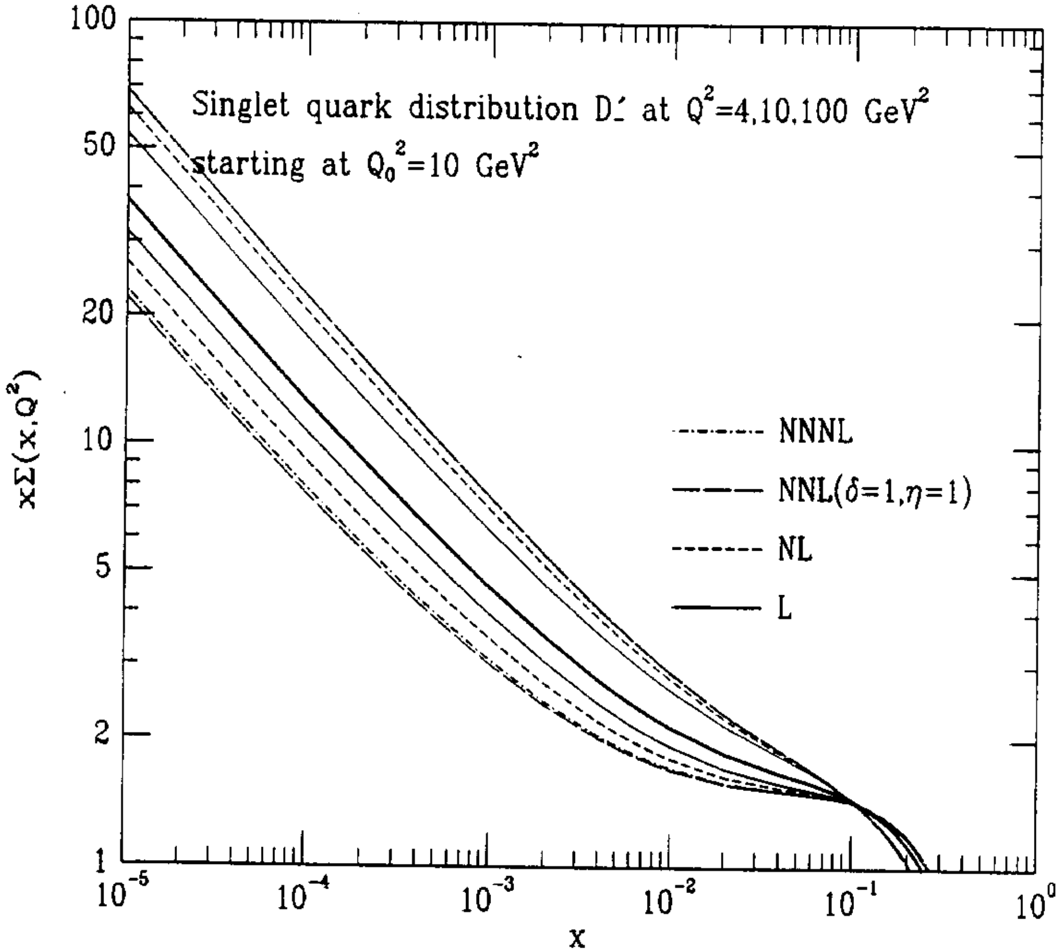

Figure 7: Evolution of D'_- gluon starting from $Q_0^2 = 10$ GeV^2

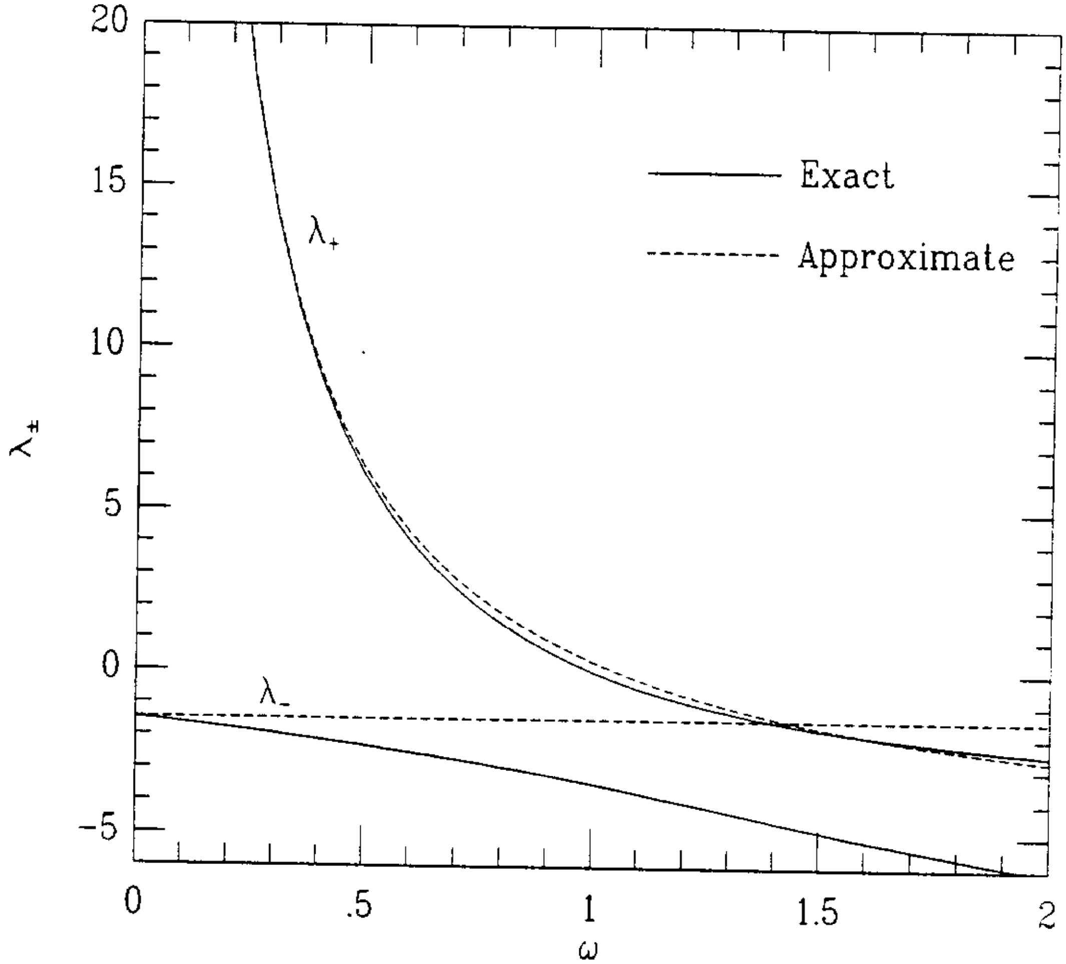

Figure 8: Exact and approximate values of λ_+ and λ_- as a function of ω

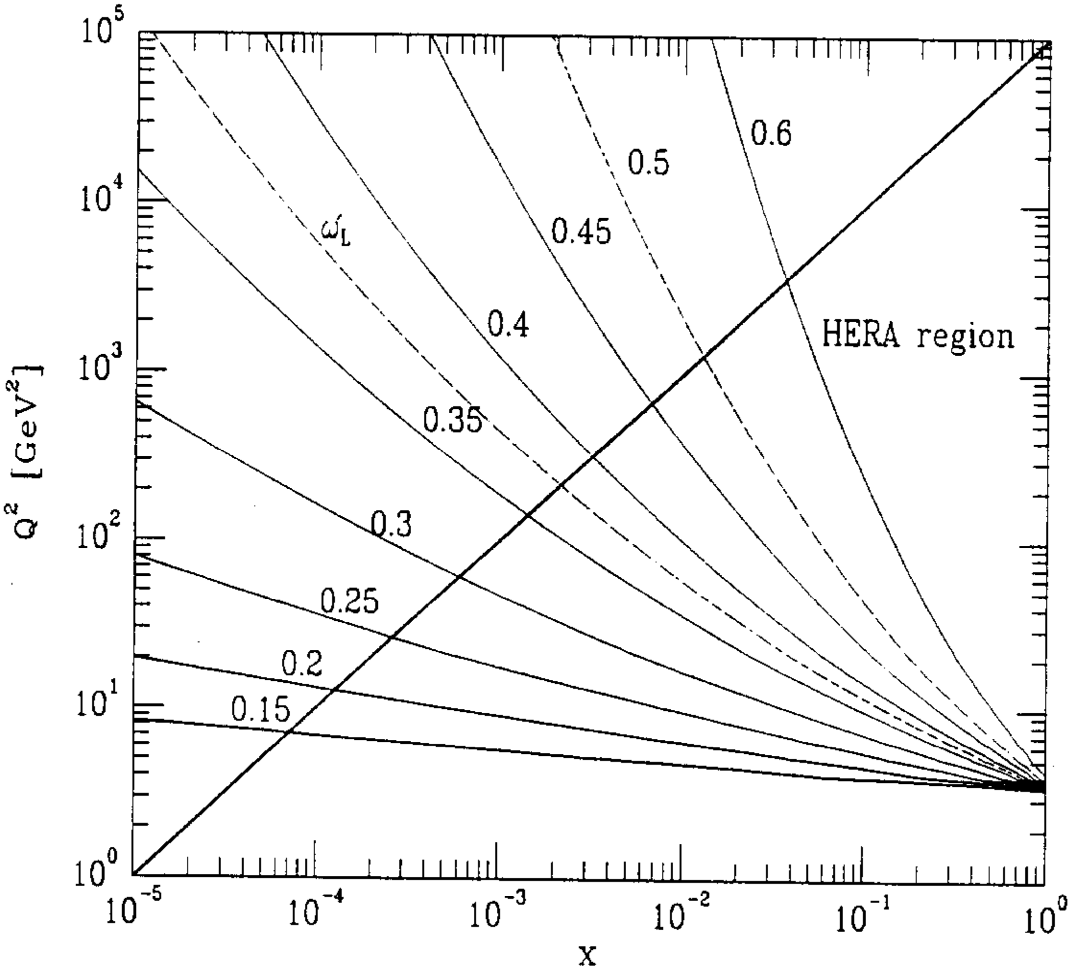

Figure 9: Contour plot showing fixed values of ω_S in Q^2, x plane

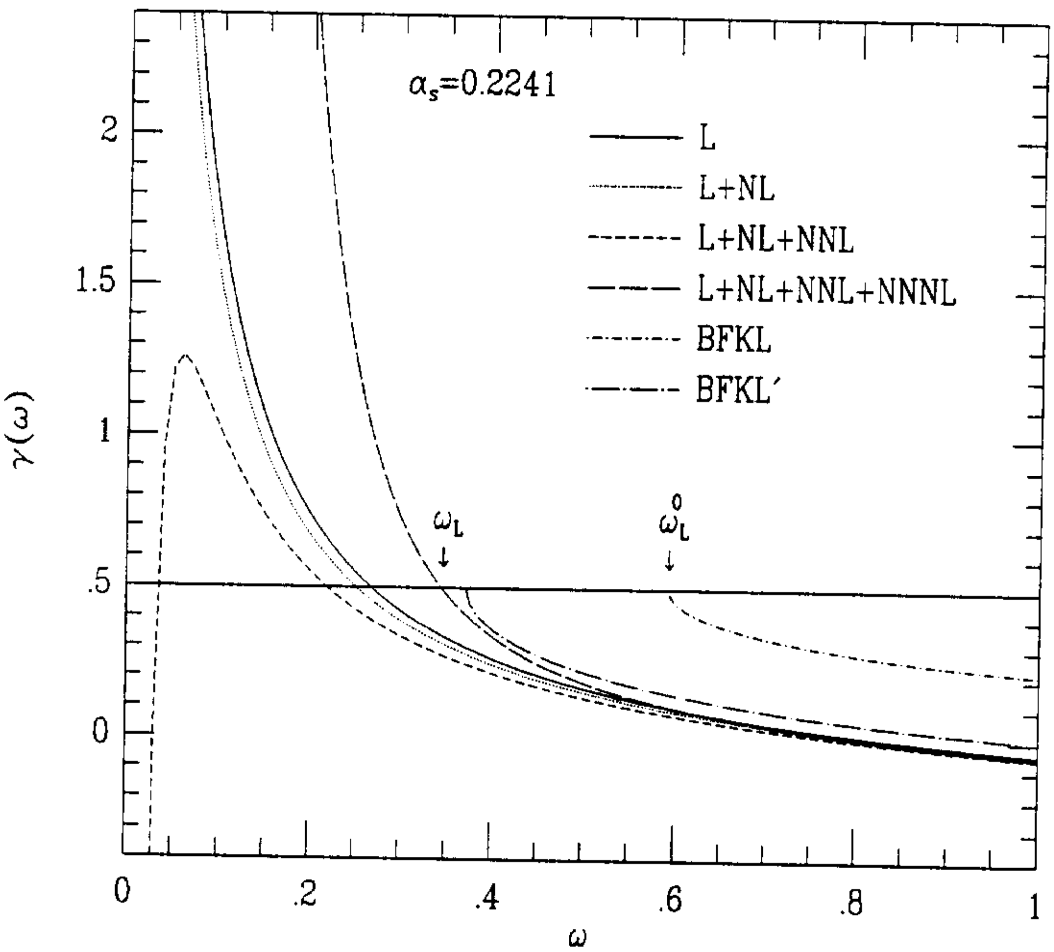

Figure 10: The GG anomalous dimension in various approximations.

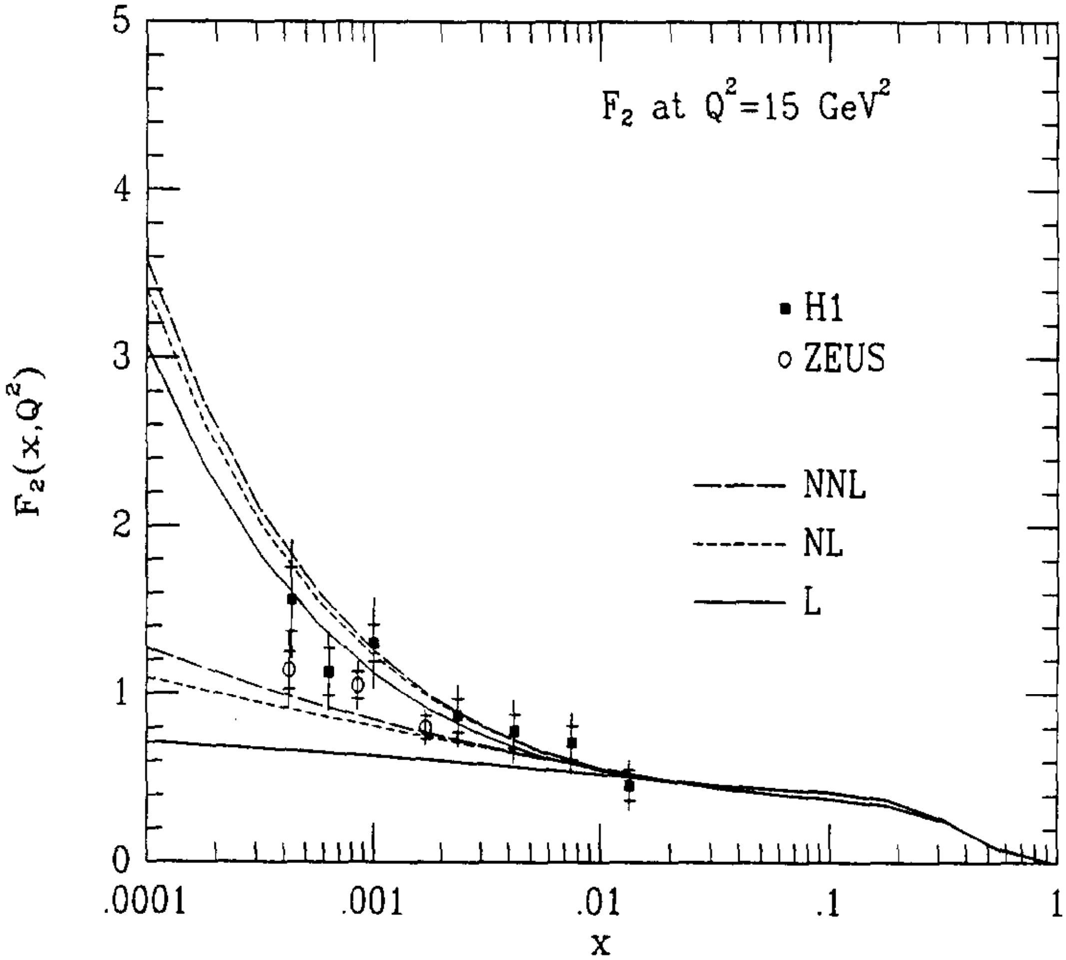

Figure 11: F_2 structure functions at $Q^2 = 15$ GeV^2

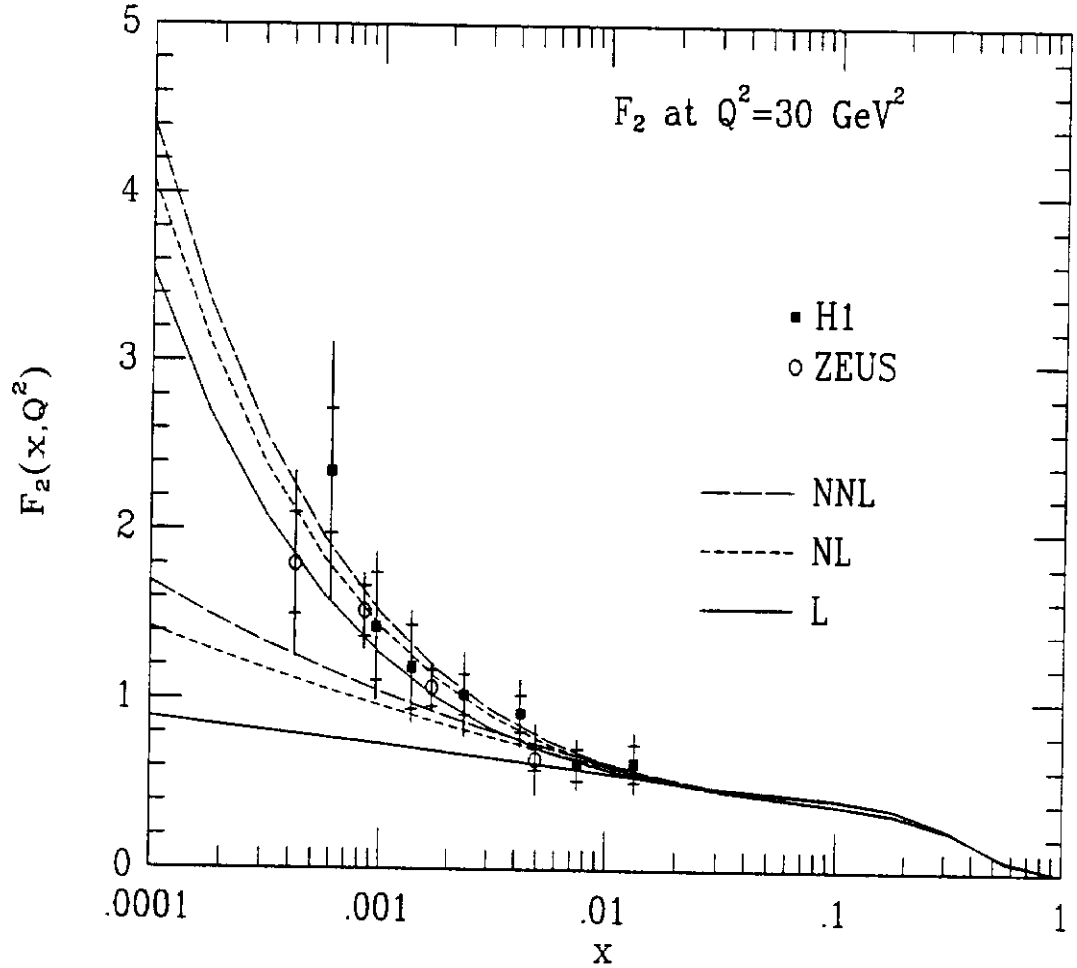

Figure 12: F_2 structure functions at $Q^2 = 30$ GeV^2

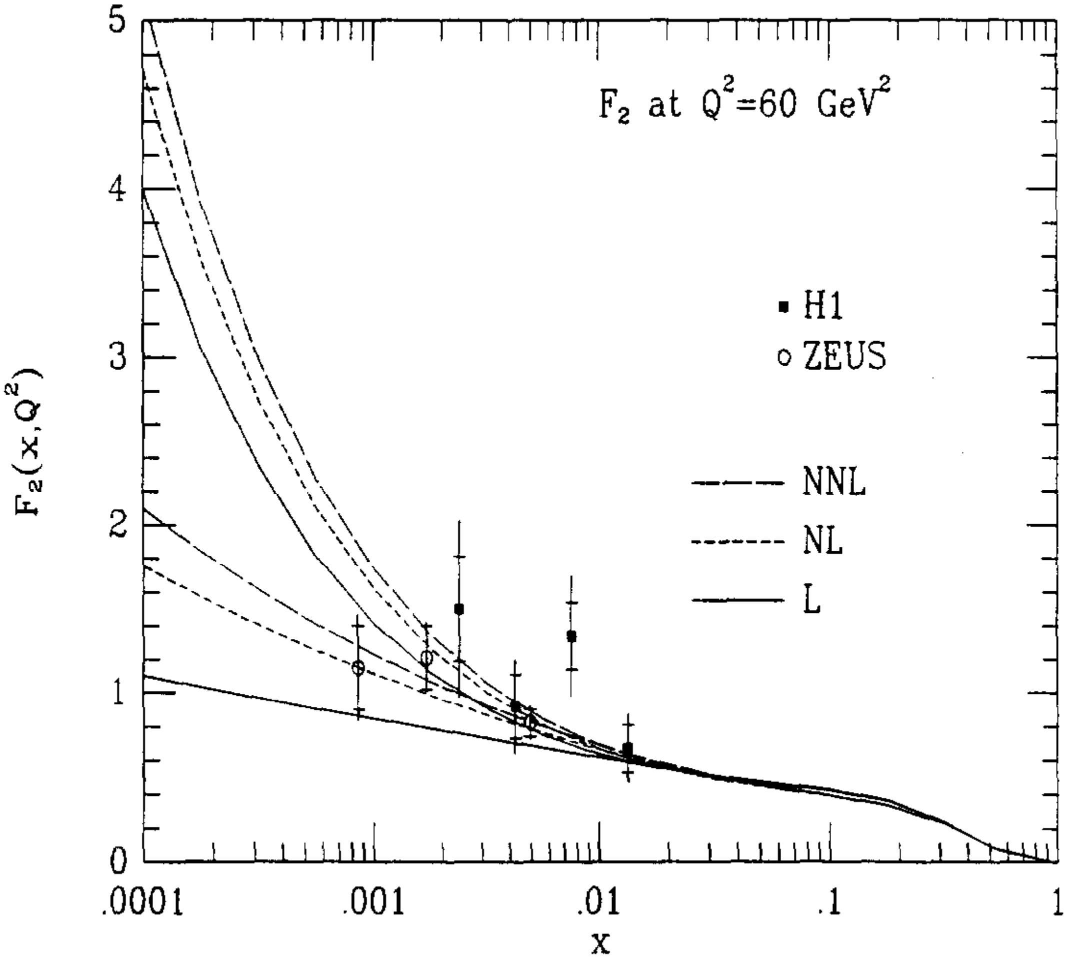

Figure 13: F_2 structure functions at $Q^2 = 60$ GeV^2

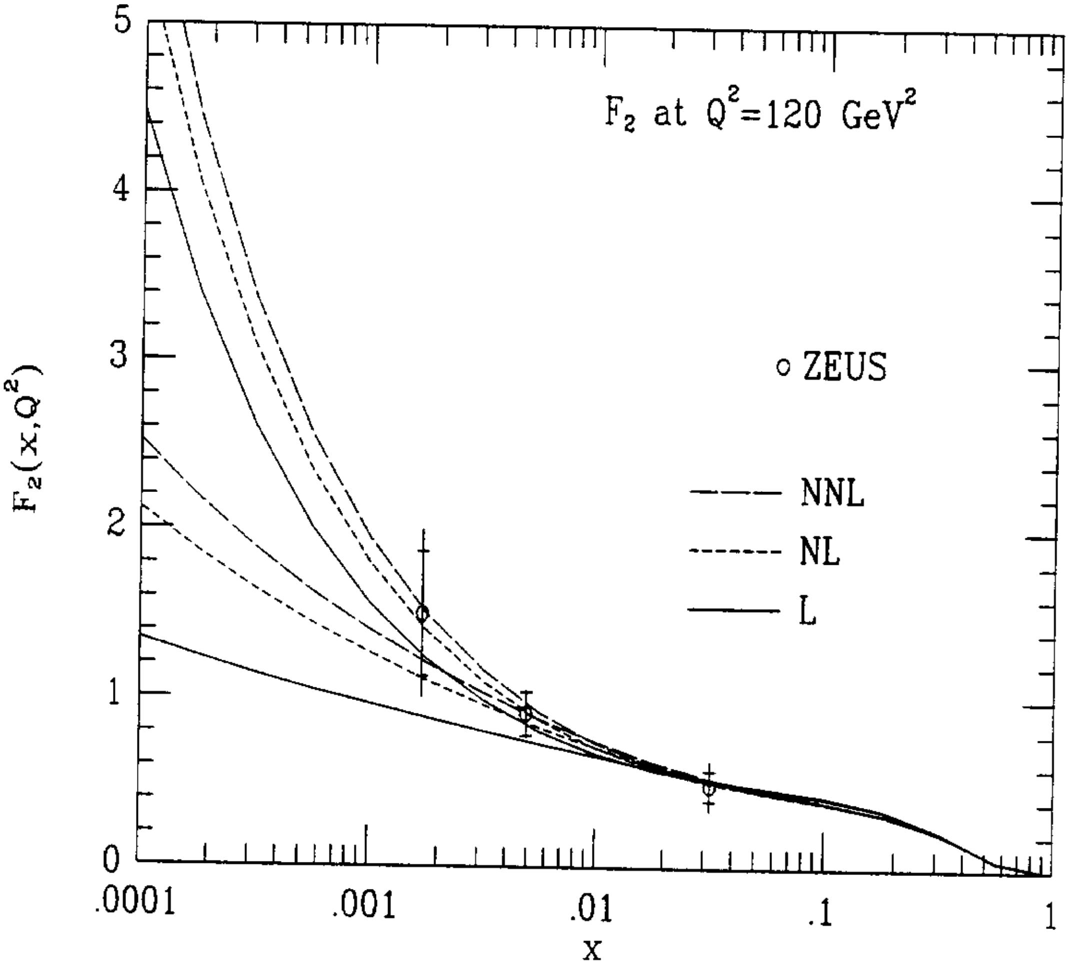

Figure 14: F_2 structure functions at $Q^2 = 120$ GeV^2